AIMS Mathematics, 9(4): 7973–8000.
DOI: 10.3934/math.2024388
Received: 12 December 2024
Revised: 26 January 2024
Accepted: 06 February 2024
Published: 26 February 2024

http://www.aimspress.com/journal/Math

Research article

Legendre spectral collocation method for solving nonlinear fractional Fredholm integro-differential equations with convergence analysis

A. H. Tedjani[1], A. Z. Amin[2], Abdel-Haleem Abdel-Aty[3], M. A. Abdelkawy[1,4,*] and Mona Mahmoud[5,*]

[1] Department of Mathematics and Statistics, College of Science, Imam Mohammad Ibn Saud Islamic University (IMSIU), Riyadh, Saudi Arabia

[2] Department of Mathematical Sciences, Faculty of Science & Technology, Universiti Kebangsaan Malaysia, 43600 UKM Bangi, Selangor, Malaysia

[3] Department of Physics, College of Sciences, University of Bisha, P.O. Box 344, Bisha 61922, Saudi Arabia

[4] Department of Mathematics, Faculty of Science, Beni-Suef University, Beni-Suef, Egypt

[5] Department of Physics, College of Science, King Khalid University, P.O. Box 9004, Abha 61413, Saudi Arabia

* **Correspondence:** Email: maohamed@imamu.edu.sa.

Abstract: The main purpose of this work was to develop a spectrally accurate collocation method for solving nonlinear fractional Fredholm integro-differential equations (non-FFIDEs). A proposed spectral collocation method is based on the Legendre-Gauss-Lobatto collocation (L-G-LC) method in which the main idea is to use Caputo derivatives and Legendre-Gauss interpolation for nonlinear FFIDEs. A rigorous convergence analysis is provided and confirmed by numerical tests. In addition, we provide some numerical test cases to demonstrate that the approach can preserve the non-smooth solution of the underlying problem.

Keywords: Legendre-Gauss-Lobatto; fractional Fredholm integro-differential equation; Caputo fractional derivative; convergence analysis; spectral method
Mathematics Subject Classification: 45Dxx, 65Mxx, 44-xx

1. Introduction

For the last three decades, researchers have been drawn to fractional calculus, which has numerous applications in engineering and physics. Fractional calculus finds utility in various fields like

image processing [1], dynamical system control theory, signal processing, electrical networks, optics, probability, statistics [2], and chemical physics. Fractional integro-differential equations, both linear and nonlinear, play a pivotal role in natural sciences and engineering, solving mathematical modeling challenges in spatiotemporal developments, biological and physical problems, epidemic modeling, and boundary value problems [3–5]. Given that analytical solutions are often elusive, the development of numerical methods for approximating solutions has become imperative.

The author in [6] has provided a solution to the dynamic model of atmospheric CO_2 concentration via a fractional mathematical model of the non-linear nature, but [7] computed the solution of some Cauchy problems and diffusion equations modeled with the Hilfer-Prabhakar fractional derivative via the Kharrat-Toma transform. The authors in [8], investigated a fractional extension of Lienard's equation by using a fractional operator with an exponential kernel.

In this paper, we present the Legendre-Gauss-Lobatto collocation (L-G-LC) method to solve the non-linear fractional Fredholm integro-differential equations (non-FFIDEs), given by:

$$D^{\alpha_1}\mathcal{Z}(\varrho) = \phi(\varrho) + \int_{-1}^{1} \sigma(\varrho, \lambda)F(\mathcal{Z}(\lambda))d\lambda, \tag{1.1}$$

with the initial conditions

$$\mathcal{Z}^{(\beta)}(0) = d_\beta, \qquad \beta = 0, 1, \tag{1.2}$$

where D^{α_1} denotes the fractional derivative of order α_1, d_β represents the initial values at $\beta = 0, 1$, and $0 < \alpha_1 < 1$.

Physical processes such as neutron transport [9], neural networks [10], population models [11], filtering and scattering [12], inverse problems [13], and disease spread [14] are all modeled using Fredholm integro-differential equations (FIDEs).

Many papers published in recent years (e.g., [15, 16]) have been devoted to discussing the FIDEs. A linear fractional Fredholm differential equation with variable coefficients has been approximated via the Taylor matrix method [17]. While [18] introduces a robust algorithm for mathematically resolving a family of two-dimensional FIDEs, the authors in [19] utilized the reproducing kernel method for approximating the solution of a nonlinear FIDE, and the fractional derivative is given in the Caputo sense in this paper. [20] used a computational method for solving a class of nonlinear Fredholm integro-differential equations of fractional order based on the second kind of Chebyshev wavelet. [21] constructed a method based on Haar wavelet approximation. The authors in [22] used an accurate numerical approach based on Wilson wavelets and the collocation method, as well as the Kumar and Sloan scheme, to numerically solve the nonlinear fractional integro-differential equations of Fredholm-Hammerstein. [23] used Taylor expansion to solve the linear fractional integro-differential equations of the Fredholm and Volterra types. It entails the n^{th}-order Taylor expansion of the unknown function at any point, yielding a system of equations for the unknown function and its m derivatives. [24] utilized a novel iterative algorithm for solving Volterra partial integro-differential problems with a weakly singular kernel. The author in [25] solves integro-differential equations (IDEs) by utilizing Jacobi-Gauss quadrature, while [26] solves fractional differential and integro-differential equations by utilizing an operational matrix method. The authors in [27] utilized the shifted Jacobi spectral collocation method to solve IDEs, while in [28] the author used the Taylor polynomial for solving non-linear IDEs. [29] solved IDEs with weakly singular kernels by utilizing spline collocation, while

in [30,31] the authors find a solution to FIDEs by applying Legendre multiwavelets and a shifted Lucas polynomial, respectively. There are several other numerical methods to consider [32, 33]. Differential collocation schemes can be obtained by either directly approximating fractional derivative operators or by recasting the governing differential equation into an equivalent integral equation [34]. Because of numerical differentiation, the integral collocation scheme has better stability properties than its differential counterpart, whereas numerical integration is inherently stable [35]. However, differential collocation schemes must use efficient integration preconditioners to overcome ill-conditioning issues when solving differential equations, which worsen as the number of collocation nodes increases.

In the last four decades, spectral methods [36–40] have been widely used in a variety of fields. Initially, Fourier-expanded spectral techniques were used in a few contexts, such as periodic boundary conditions and simple geometric areas. They have recently advanced theoretically and been used as powerful techniques to solve a variety of problems. When compared to other numerical techniques, spectral techniques have a superior character based on thoroughness and exponential averages of convergence. The fundamental step in all spectral techniques is to express the problem solution as a finite series of several functions. Spectral methods include many types, such as collocation [41–44], tau [45], Galerkin [46], and Petrov-Galerkin [47]. The coefficients will then be chosen to minimize the absolute error. During this time, the numerical solution in the spectral collocation technique will be implemented to nearly satisfy IDEs (see [48–50]). On the other hand, at selection points, the residuals may be permitted to be zero. The collocation approach has been successfully applied in a wide range of scientific and engineering areas due to its obvious advantages. Because their global nature fits well with the nonlocal definition of fractional operators, spectral collocation methods are promising candidates for solving fractional differential equations.

The main goal of the paper is to use the L-G-LC method for approximating non-FFIDEs with L-GL interpolation nodes. We estimate the residuals of the aforementioned problem by using a finite expansion of a shifted Legendre polynomial for independent variables and L-GL quadrature points to approximate the solution of an equation. When these equations are combined with the initial conditions, they yield an algebraic system of (N+1) equations that can be solved. In addition, we investigate the convergence of approximation solutions. To demonstrate the method's accuracy, numerical simulations of some non-FFIDEs are presented.

This paper is structured as follows: Section 2 contains some preliminary information about FDEs. In Section 3, we utilized the L-G-LC method for building a technique to solve nonlinear FFIDEs. Section 4 discusses the spectral collocation method's convergence analysis. Numerical simulations are presented in Section 5 to ensure the effectiveness of the proposed method. Some observations and conclusions are provided in Section 6.

2. Fractional calculus

This section introduces the main definitions used in the following section as the left and right Caputo (RL-C) definitions. [42] gives the RL-C derivative D_1^{α} of order α_1 as

$$D_{+}^{\alpha_1}\mathcal{Z}(\varrho) = \frac{1}{\Gamma(\eta-\alpha_1)}\left(\int_0^{\varrho}(\varrho-\kappa)^{\eta-\alpha_1-1}\mathcal{Z}^{(\eta)}(\kappa)d\kappa\right), \quad \eta-1<\alpha_1\leq\eta,\ \varrho>0. \tag{2.1}$$

$$D_{-}^{\alpha_1}\mathcal{Z}(\varrho) = \frac{(-1)^{\eta}}{\Gamma(\eta-\alpha_1)}\left(\int_{\varrho}^{L}(\kappa-\varrho)^{\eta-\alpha_1-1}\mathcal{Z}^{(\eta)}(\kappa)d\kappa\right), \quad \eta-1<\alpha_1\leq\eta,\ \varrho>0. \tag{2.2}$$

The operator $D_{\pm}^{\alpha_1}$ satisfies the following properties:

$$D_{\pm}^{\alpha_1}I_{\pm}^{\alpha_1}\mathcal{Z}(\kappa) = \mathcal{Z}(\kappa)I_{\pm}^{\alpha_1}D_{\pm}^{\alpha_1}\mathcal{Z}(\kappa) = -\sum_{\varepsilon=0}^{\lceil\alpha_1\rceil-1}\mathcal{Z}^{(\varepsilon)}(0^{+})\frac{\kappa^{\varepsilon}}{\varepsilon!}+\mathcal{Z}(\kappa), \tag{2.3}$$

where $D^{\alpha_1}\pm$ and $I\pm^{\alpha_1}$ are operators of left and right Caputo differential and integral, respectively.

$$D_{+}^{\alpha_1}\kappa^{\varepsilon} = \begin{cases} 0, & \text{for } \varepsilon\in\mathbb{N}_0 \text{ and } \varepsilon<\lceil\alpha_1\rceil,\\ \frac{\Gamma(\varepsilon+1)}{\Gamma(\varepsilon+1-\alpha_1)}\kappa^{\varepsilon-\alpha_1}, & \text{for } \varepsilon\in N_0 \text{ and } \varepsilon\geq\lceil\alpha_1\rceil \text{ or } \varepsilon\notin\mathbb{N} \text{ and } \varepsilon>\lfloor\alpha_1\rfloor, \end{cases} \tag{2.4}$$

where $\lfloor\alpha_1\rfloor$ and $\lceil\alpha_1\rceil$ denote the floor and ceiling functions, respectively, while $\mathbb{N} = \{1,2,\ldots\}$ and $\mathbb{N}_0 = \{0,1,2,\ldots\}$.

For $\alpha_1 > 0$, the fractional integrals of order α_1 [42], both left-sided and right-sided, are specified as follows:

$$I_{+}^{\alpha_1}\mathcal{Z}(\varrho) = \frac{1}{\Gamma(\alpha_1)}\int_{0}^{\varrho}(\varrho-\kappa)^{\alpha_1-1}\mathcal{Z}(\kappa)d\kappa, \tag{2.5}$$

$$I_{-}^{\alpha_1}\mathcal{Z}(\varrho) = \frac{1}{\Gamma(\alpha_1)}\int_{\varrho}^{L}(\kappa-\varrho)^{\alpha_1-1}\mathcal{Z}(\kappa)d\kappa. \tag{2.6}$$

3. The spectral collocation method

In the next section, we will propose a Legendre spectral collocation (LSC) method for solving Eq (1.1).

3.1. L-GL interpolation

The Legendre polynomials $\mathcal{L}_{\kappa}(\varrho)$, $\kappa = 0, 1\ldots$, follow the Rodrigues formula [51]:

$$\mathcal{L}_{\kappa}(\varrho) = \frac{(-1)^{\kappa}}{2^{\kappa}\kappa!}D^{\mathcal{Z}}((1-\varrho^2)^{\kappa}). \tag{3.1}$$

Furthermore, $\mathcal{L}_{\kappa}(\varrho)$ aligns with a polynomial of degree κ, resulting in the pth derivative of $\mathcal{L}_{\kappa}(\varrho)$ as:

$$\mathcal{L}_{\kappa}^{(p)}(\varrho) = \sum_{\rho=0(\kappa+\rho=even)}^{\kappa-p}C_p(\kappa,\rho)\mathcal{L}_{\rho}(\varrho), \tag{3.2}$$

where

$$C_p(\kappa,\rho) = \frac{2^{p-1}(2\rho+1)\Gamma(\frac{p+\kappa-\rho}{2})\Gamma(\frac{p+\kappa+\rho+1}{2})}{\Gamma(p)\Gamma(\frac{2-p+\kappa-\rho}{2})\Gamma(\frac{3-p+\kappa+\rho}{2})}.$$

Orthogonality is attained through the execution of the subsequent procedures:

$$(\mathcal{L}_\kappa(\varrho), \mathcal{L}_l(\varrho))_\chi = \int_{-1}^{1} \mathcal{L}_\kappa(\varrho)\mathcal{L}_l(\varrho)\,\chi(\varrho) = h_\kappa \alpha_{l\kappa}, \tag{3.3}$$

where $\chi(\varrho) = 1$, $h_\kappa = \frac{2}{2\kappa+1}$.

The L-GL quadrature method was employed to effectively compute the integrals presented earlier. For any $\mathcal{Z} \in S_{2\nu_1-1}$ on the interval $[-1, 1]$, we can express:

$$\int_{-1}^{1} \mathcal{Z}(\varrho)d\varrho = \sum_{\varepsilon=0}^{\nu_1} \varpi_{\nu_1,j}\mathcal{Z}(\varrho_{\nu_1,\varepsilon}). \tag{3.4}$$

For instance, contemplate the discrete inner product:

$$(\mathcal{Z}, \mathcal{Z})_w = \sum_{\varepsilon=0}^{\nu_1} \mathcal{Z}(\varrho_{\nu_1,\varepsilon})\,\mathcal{Z}(\varrho_{\nu_1,\varepsilon})\,\varpi_{N,j}. \tag{3.5}$$

In the case of L-GL, we ascertain that [52] $\varrho_{\nu_1,0} = -1$, $\varrho_{\nu_1,\nu_1} = 1$, $\varrho_{\nu_1,\varepsilon}$ and $(\varepsilon = 1, \cdots, \nu_1 - 1)$ are the zeros of $(l_{\nu_1}(\varrho))'$, and $\varpi_{\nu_1,\varepsilon} = \frac{2}{\nu_1(\nu_1+1)(\mathcal{L}_{\nu_1}(\varrho_{\nu_1,\varepsilon}))^2}$, where $\varpi_{\nu_1,\varepsilon}$ (with $0 \le \varepsilon \le \nu_1$) and $\varrho_{\nu_1,\varepsilon}$ (with $0 \le \varepsilon \le \nu_1$) serve as the Christoffel numbers and nodes within the interval $[-1, 1]$, respectively. To apply these polynomials in the range $\varrho \in (0, l_1)$, we introduce a shifted Legendre polynomials (SLPs) by utilizing $\varrho = \dfrac{2\varrho}{l_1} - 1$.

If we denote by $\mathcal{L}_{l_1,\rho}(\varrho)$ the SLP $\mathcal{L}_\rho\left(\dfrac{2\varrho}{l_1} - 1\right)$, then $\mathcal{L}_{l_1,\rho}(\varrho)$ can be obtained as [51]:

$$(\rho + 1)\mathcal{L}_{l_1,\rho+1}(\varrho) = (2\rho + 1)(\frac{2\varrho}{l_1} - 1)\mathcal{L}_{l_1,\rho}(\varrho) - \rho\mathcal{L}_{l_1,\rho-1}(\varrho), \qquad \rho = 1, 2, \cdots. \tag{3.6}$$

The analytical representation of the SLP denoted as $\mathcal{L}_{l_1,\rho}(\varrho)$ of degree ρ is expressed as follows:

$$\mathcal{L}_{l_1,\rho}(\varrho) = \sum_{\kappa=0}^{\rho} (-1)^{\rho+\kappa} \frac{(\rho + \kappa)!}{(\rho - \kappa)!(\kappa!)^2\,\mathcal{L}^\kappa} \varrho^\kappa. \tag{3.7}$$

The condition of orthogonality is expressed as:

$$\int_0^l \mathcal{L}_{l_1,\varepsilon}(\varrho)\mathcal{L}_{l_1,\kappa}(\varrho)w_{l_1}(\varrho)d\varrho = \hbar_\kappa\,\alpha_{\varepsilon\kappa}, \tag{3.8}$$

where $w_{l_1}(\varrho) = 1$ and $\hbar_\kappa = \dfrac{l_1}{2\kappa + 1}$.

In terms of SLPs, a square integrable function $\mathcal{Z}(\varrho)$ in the interval $(0, l)$ can be expressed as:

$$\mathcal{Z}(\varrho) = \sum_{\varepsilon=0}^{\infty} e_\varepsilon \mathcal{L}_{l_1,\varepsilon}(\varrho), \tag{3.9}$$

where the coefficients e_ε are:

$$e_\varepsilon = \frac{1}{\hbar_\varepsilon}\int_0^l \mathcal{Z}(\varrho)\mathcal{L}_{l_1,\varepsilon}(t)w_{l_1}(\varrho)d\varrho, \quad \varepsilon = 0, 1, 2, \cdots . \tag{3.10}$$

The initial $(\nu_1 + 1)$ terms of the SLPs find application in practical scenarios. Consequently, $\mathcal{Z}(\varrho)$ is formulated as follows:

$$\mathcal{Z}_{\nu_1}(\varrho) \simeq \sum_{\varepsilon=0}^{\nu_1} e_\varepsilon \mathcal{L}_{l_1,\varepsilon}(\varrho). \tag{3.11}$$

3.2. LSC scheme

We used the L-G-C method to solve non-FFIDEs with initial conditions,

$$D^{\alpha_1}\mathcal{Z}(\varrho) = \phi(\varrho) + \int_{-1}^{1} \sigma(\varrho, \lambda)F(\mathcal{Z}(\lambda))d\lambda, \qquad 0 < \alpha_1 < 1, \tag{3.12}$$

with the initial conditions

$$\mathcal{Z}^{(\alpha)}(0) = d_\beta, \qquad \beta = 0, 1. \tag{3.13}$$

The LSC method for Eq (3.12) is to explore the approximate solution in the form,

$$\mathcal{Z}_{\nu_1}(\varrho) = \sum_{\varepsilon=0}^{\nu_1} e_\varepsilon \mathcal{L}_\varepsilon(\varrho). \tag{3.14}$$

As a result, inserting Eq (3.14) into Eq (3.12),

$$D^{\alpha_1}\mathcal{Z}_{\nu_1}(\varrho) = I_{\varrho,\nu_1}\phi(\varrho) + \int_{-1}^{1} I_{\varrho,\nu_1}I_{\lambda,\nu_1}[\sigma(\varrho, \lambda)F(\mathcal{Z}(\lambda))]d\lambda, \qquad 0 < \alpha_1 < 1, \tag{3.15}$$

where I_{ϱ,ν_1}, I_{λ,ν_1} are Legendre-Gauss interpolation operators.

Now, we describe how we implemented our form Eq (3.15) by utilizing the Legendre-Gauss interpolation, which serves as the foundation for our scheme, setting,

$$I_{\varrho,\nu_1}I_{\lambda,\nu_1}[\sigma(\varrho, \lambda)F(\mathcal{Z}(\lambda))] = \sum_{\varepsilon=0}^{\nu_1}\sum_{\imath=0}^{\nu_1} e_{\varepsilon\imath}\mathcal{L}_\varepsilon(\varrho)\mathcal{L}_\imath(\lambda), \tag{3.16}$$

we can obtain

$$\int_{-1}^{1} I_{\varrho,\nu_1}I_{\lambda,\nu_1}[\sigma(\varrho, \lambda)F(\mathcal{Z}(\lambda))]d\lambda = \sum_{\varepsilon=0}^{\nu_1}\sum_{\imath=0}^{\nu_1} e_{\varepsilon\imath}\mathcal{L}_\varepsilon(\varrho)\int_{-1}^{1}\mathcal{L}_\imath(\lambda)d\lambda = \omega\sum_{\varepsilon=0}^{\nu_1} e_{\varepsilon,0}\mathcal{L}_\varepsilon(\varrho), \tag{3.17}$$

where $\omega = \sum_{\imath=0}^{\nu_1} e_\imath(\int_{-1}^{1}\mathcal{L}_\imath(\lambda)d\lambda)$.
The fractional derivative of $\mathcal{Z}_{\nu_1}(\varrho)$ is then evaluated as

$$D^{\alpha_1}\mathcal{Z}_{\nu_1}(\varrho) = \sum_{\varepsilon=0}^{\nu_1} e_\varepsilon D^{\alpha_1}(\mathcal{L}_\varepsilon(\varrho)) = \sum_{\varepsilon=0}^{\nu_1} e_\varepsilon\xi_\varepsilon(\varrho). \tag{3.18}$$

Utilizing Eqs (3.18) and (3.17), we can express Eq (3.12) as:

$$\sum_{\varepsilon=0}^{\nu_1} e_\varepsilon \xi_\varepsilon(\varrho) = \omega \sum_{\varepsilon=0}^{\nu_1} e_{\varepsilon,0} \mathcal{L}_\varepsilon(\varrho) + \sum_{\varepsilon=0}^{\nu_1} \nu_1^\varepsilon \mathcal{L}_\varepsilon(\varrho), \tag{3.19}$$

where $\nu_1^\varepsilon = \sum_{\varepsilon=0}^{\nu_1} \phi(\varrho)\varpi_\varepsilon L_\varepsilon(\varrho)$.

Merging Eqs (3.14) and (3.13), we get

$$\sum_{\varepsilon=0}^{\nu_1} e_\varepsilon D^\beta \mathcal{L}_{\mathcal{L},\varepsilon}(0) = \phi_\beta, \qquad \beta = 0, 1. \tag{3.20}$$

Conversely, we can formulate

$$(-1)^\varepsilon e_\varepsilon = \phi_0, \tag{3.21}$$

$$\sum_{\varepsilon=0}^{\nu_1} \frac{(-1)^{\varepsilon-1}\Gamma(\varepsilon+1)(\varepsilon+1)}{\mathcal{L}(\varepsilon-1)!\Gamma(2)} e_\varepsilon = \phi_1. \tag{3.22}$$

Equations (3.21)–(3.23) are equivalent to a discretized system of $(\nu_1 + 1)$ algebraic equations with the unknowns e_ε, $\rho = 0, \cdots, \nu_1$,

$$\begin{cases} (-1)^\varepsilon e_\varepsilon = \phi_0, \\ \sum\limits_{\varepsilon=0}^{\nu_1} \frac{(-1)^{\varepsilon-1}\Gamma(\varepsilon+1)(\varepsilon+1)}{\mathcal{L}(\varepsilon-1)!\Gamma(2)} e_\varepsilon = \phi_1, \\ \sum\limits_{\varepsilon=0}^{\nu_1} e_\varepsilon \xi_\varepsilon(\varrho) = \alpha_1 \sum_{\varepsilon=0}^{\nu_1} e_{\varepsilon,0} \mathcal{L}_\varepsilon(\varrho) + \sum_{\varepsilon=0}^{\nu_1} W_\varepsilon L_\varepsilon(\varrho). \end{cases} \tag{3.23}$$

At last, the linear system of (ν_1+1) algebraic equations generated are solved automatically and quickly, and can be solved by Newton's iterative method. In our implementation, this system has been solved using the Mathematica function. As a result, $\mathcal{Z}_{\nu 1}(\varrho)$ can be calculated in closed form.

4. Convergence analysis

A discussion of error analysis is included, as well as some useful lemmas.

Assume$P_N : L^2(I) \to \varrho_N$ to be the L^2 orthogonal projection, as defined by [52]

$$(P_N \mathcal{Z}(\varrho) - \mathcal{Z}(\varrho), \rho) = 0, \qquad \forall \rho \in \mathcal{Z}_N.$$

Here are some definitions of weighted Hilbert spaces. For a nonnegative integer η, define [51, 52]

$$H^\eta(-1, 1) = \{\mathcal{Z} : \partial_\varrho^\iota \mathcal{Z} \in L^2(-1, 1), 0 \le i \le \eta\},$$

whereas $\partial_\varrho^\iota \mathcal{Z}(\varrho) = \frac{\partial^\iota \mathcal{Z}(\varrho)}{\partial \varrho^\iota}$, related to the norm and semi-norm as follows:

$$\| \mathcal{Z} \|_\eta = (\sum_{\iota=0}^{\eta} \| \partial_\varrho^\iota \mathcal{Z} \|^2)^{\frac{1}{2}}$$

$$\mathcal{Z}_\eta = \| \partial_\varrho^\eta \mathcal{Z} \| .$$

Lemma 1. Assume I_N denotes the polynomial of degree N interpolating $\mathcal{Z}$ at one of these point sets, and that the interpolation error is estimated as $\mathcal{Z} - I_N\mathcal{Z}$ in the norms of the Sobolev spaces $H^1(-1,1)$. When $u \in H^\eta(-1,1)$ and $\eta \geq 1$, the relationship holds, as indicated by [52].

$$\| \mathcal{Z} - I_N\mathcal{Z} \|_{L^2(-1,1)} \leq CN^{-\eta} \mid \mathcal{Z} \mid_{H^{\eta,N}(-1,1)} . \tag{4.1}$$

Lemma 2. Let $\mathcal{Z} \in H^\eta(I), \quad I \equiv (-1,1)$. The following estimates are satisfied by the interpolation of $\mathcal{Z}$ $(I_N\xi)$ computed at any point of Jacobi Gauss points (Gauss-Radau points, Gauss-lobatto, or Gauss) [52]:

$$\| \mathcal{Z}^{'}(\varrho) - (I_N\mathcal{Z}(\varrho))^{'} \|_{L^2_{(I)}} \leq CN^{1-\eta} \mid \mathcal{Z} \mid_{H^1(I)} . \tag{4.2}$$

Lemma 3. Consider $e(x) = \mathcal{Z}(\varrho) - \mathcal{Z}N(\varrho)$ to represent the error function of the solution. The subsequent inequality is applicable in this context:

$$\|e\| \leq \sum_{\ell=1}^{4} \|B_\ell\| \tag{4.3}$$

where

$B_1 = \frac{1}{\Gamma(1-\alpha_1)} I_{\varrho,N} \int_0^{\varrho} (\varrho - \lambda)^{-\alpha_1} \Big(\mathcal{Z}^{'}(\alpha_1) - (I_{\lambda,N}\mathcal{Z}(\lambda))^{'} \Big) d\lambda$

$B_2 = I_{\varrho,N} \int_{-1}^{1} (I - I_{\lambda,N}) \Big[\sigma(\varrho,\lambda) F(\mathcal{Z}(\lambda)) \Big] d\lambda$

$B_3 = I_{\varrho,N} \int\limits_{-1}^{1} I_{\lambda,N} \Big[\sigma(\varrho,\lambda) F(\mathcal{Z}(\lambda)) - \sigma(\varrho,\lambda) F(\mathcal{Z}_N(\lambda)) \Big] d\lambda.$

Proof. By using the Caputo definition, we write the equation of non-FFIDEs as follows:

$$\frac{1}{\Gamma(1-\alpha_1)} I_{\varrho,N} \int_0^{\varrho} (\varrho - \lambda)^{-\alpha_1} \mathcal{Z}^{'}(\lambda) d\lambda = I_{\varrho,N}\phi(\varrho) + I_{\varrho,N} \int_{-1}^{1} \sigma(\varrho,\lambda) F(\mathcal{Z}(\lambda)) d\lambda, \qquad 0 < \alpha_1 < 1 \tag{4.4}$$

and when utilizing the approximate solution we have,

$$\frac{1}{\Gamma(1-\alpha_1)} I_{\varrho,N} \int_0^{\varrho} (\varrho - \lambda)^{-\alpha_1} I_{\lambda,N} \mathcal{Z}^{'}(\lambda) d\lambda = I_{\varrho,N}\phi(\varrho) + \int_{-1}^{1} I_{\varrho,N} I_{\lambda,N} [\sigma(\varrho,\lambda) F(\mathcal{Z}_N(\lambda))] d\lambda. \tag{4.5}$$

Subtracting (4.5) from (4.4) yields

$$\begin{aligned} e(\varrho) = \frac{1}{\Gamma(1-\alpha_1)} I_{\varrho,N} \int_0^{\varrho} (\varrho - \lambda)^{-\alpha_1} \mathcal{Z}^{'}(\lambda) d\lambda - \frac{1}{\Gamma(1-\alpha_1)} I_{\varrho,N} \int_0^{\varrho} (\varrho - \lambda)^{-\alpha_1} I_{\lambda,N} \mathcal{Z}^{'}(\lambda) d\lambda \\ + I_{\varrho,N} \int_{-1}^{1} \Big[\sigma(\varrho,\lambda) F(\mathcal{Z}(\lambda)) - I_{\lambda,N} [\sigma(\varrho,\lambda) F(\mathcal{Z}_N(\lambda))] \Big] d\lambda \end{aligned} \tag{4.6}$$

hence

$$\begin{aligned} e(t) = \frac{1}{\Gamma(1-\alpha_1)} I_{\varrho,N} \int_0^{\varrho} (\varrho - \lambda)^{-\alpha_1} (\mathcal{Z}^{'}(\alpha_1) - (I_{\varrho,N}\mathcal{Z}(\lambda))^{'}) d\lambda + I_{\varrho,N} \int_{-1}^{1} (I - I_{\lambda,N}) \sigma(\varrho,\lambda) F(\mathcal{Z}(\lambda)) d\lambda \\ + I_{\varrho,N} \int_{-1}^{1} I_{\lambda,N} \Big[\sigma(\varrho,\lambda) F(\mathcal{Z}(\lambda)) - \sigma(\varrho,\lambda) F(\mathcal{Z}_N(\lambda)) \Big] d\lambda. \end{aligned} \tag{4.7}$$

The desired result can be obtained directly from the above.

4.1. Error analysis

Theorem 1. Let $I_N\mathcal{Z}(\varpi)$ be the spectral approximate and let $\mathcal{Z}(\varpi)$ be the exact solution of the equation of non-FFIDEs and, consequently we obtain

$$\begin{aligned} \| E_N \|_{L^2(I)} \leq \zeta C_6 N^{1-\eta} |\mathcal{Z}|_{H^1(I)} + c\sqrt{\frac{(N-\eta+1)!}{N!}}(N+\eta)^{-(\eta+1)/2}\Big[|F(\mathcal{Z}(\cdot))|_{H^1(I)} + |\mathcal{Z}|_{H^1(I)}\Big] \\ + LM \| E_N \| . \end{aligned} \tag{4.8}$$

Proof. In the ϱ-direction, the interpolation operator is formally defined as $I_{\varrho,N} : C(-1,1) \to P_N$ for any $\mathcal{Z}(\varrho) \in C(-1,1)$

$$I^{\nu_1,\nu}_{\varrho,N}\mathcal{Z}(\varrho^{\nu_1,\nu}_\ell) = \mathcal{Z}(\varrho^{\nu_1,\nu}_\ell), \quad 0 \leq \ell \leq N. \tag{4.9}$$

The Jacobi polynomial is reduced to the Legender polynomial $L_n(\varrho)$ in the special case on condition that $\nu_1 = \nu = 0$. We can write $\varrho_\ell = \varrho^{0,0}_\ell$, $\phi_\ell = \phi^{0,0}_\ell$, and $I_{\varrho,N} = I^{0,0}_{\varrho,N}$. Equation (4.10) can be formulated utilizing Lemma 3 and the Gronwall inequality:

$$\| e(x) \|_{L_2} \leq \| B_1 \|_{L_2} + \| B_2 \|_{L_2} + \| B_3 \|_{L_2} . \tag{4.10}$$

We compute B_1 using Lemmas 2 and 3, and the Cauchy-Schwarz inequality, where $0 < \alpha_1 < 1$,

$$\begin{aligned} \| B_1 \| &= \frac{1}{\Gamma(1-\alpha_1)} I_{\varrho,N} \left\| \int_0^{\varrho} (\varrho-\lambda)^{-\alpha_1} (\varphi^{'}(\lambda) - (I_{\lambda,N}\mathcal{Z}(\lambda))^{'}) d\lambda \right\|_{L_2(I)}, \\ &= \frac{1}{\Gamma(1-\alpha_1)} \sum_{\ell=0}^{N} \varpi_\ell \left\| \int_0^{\varrho_\ell} (\varrho_\ell-\lambda)^{-\alpha_1} (\mathcal{Z}^{'}(\lambda) - (I_{\lambda,N}\mathcal{Z}(\lambda))^{'}) d\lambda \right\|_{L_2(I)}, \\ &\leq \frac{1}{\Gamma(1-\alpha_1)} \sum_{\ell=0}^{N} \varpi_\ell \int_0^{\varrho_\ell} (\varrho_\ell-\lambda)^{-\alpha_1} d\lambda \left\| (\mathcal{Z}^{'}(\lambda) - (\lambda, I_{\lambda,N}\mathcal{Z}(\lambda))^{'}) \right\|_{L_2(I)}, \\ &\leq \zeta \left\| (\mathcal{Z}^{'}(\lambda) - (I_N\mathcal{Z}(\lambda))^{'}) \right\|_{\infty}, \\ &\leq \zeta C_6 N^{1-\eta} |\mathcal{Z}|_{H^1(I)} . \end{aligned} \tag{4.11}$$

The quantity $|B_2|$ is subsequently approximated as follows:

$$\begin{aligned} \| B_2 \| &= \left\| I_{\varrho,N} \int_{-1}^{1} (I - I_{\lambda,N})[\sigma(\varrho,\lambda)F(\mathcal{Z}(\lambda))] d\lambda \right\| \\ &= \Big[\sum_{|\iota|_\infty \leq N} \varpi_\iota \Big(\int_{-1}^{1} (I - I_{\lambda,N})\sigma(\varrho_\iota,\lambda)F(\mathcal{Z}(\lambda)) d\lambda \Big)^2 \Big]^{\frac{1}{2}}. \end{aligned} \tag{4.12}$$

By using the Cauchy inequality, we can get

$$\begin{aligned} \| B_2 \| &\leq \Big[\sum_{|\iota|_\infty \leq N} \varpi_\iota \int_{-1}^{1} \Big| (I - I_{\lambda,N})\sigma(\varrho_\iota,\lambda)F(\mathcal{Z}(\lambda)) \Big|^2 d\lambda \Big]^{\frac{1}{2}} \\ &\leq \Big(\sum_{|\iota|_\infty \leq N} \varpi_\iota \Big)^{\frac{1}{2}} \max_{|\iota|_\infty \leq N} \Big(\int_{-1}^{1} \Big| (I - I_{\lambda,N})\sigma(\varrho_\iota,\lambda)F(\mathcal{Z}(\lambda)) \Big|^2 d\lambda \Big)^{\frac{1}{2}}. \end{aligned} \tag{4.13}$$

Hence,

$$\| B_2 \| \leq c \sqrt{\frac{(N-\eta+1)!}{N!}} (N+\eta)^{-(\eta+1)/2} |F(\mathcal{Z}(\cdot))|. \tag{4.14}$$

We have now determined an estimate for the term $|B_3|$. The Legendre-Gauss integration formula (3.3) has been applied to achieve this result.

$$\begin{aligned} \| B_3 \| &= \left\| I_{\varrho,N} \int_{-1}^{1} I_{\lambda,N} [\sigma(\varrho,\lambda) F(\mathcal{Z}(\lambda)) - \sigma(\varrho,\lambda) F(\mathcal{Z}_N(\lambda))] d\lambda \right\| \\ &= \Big[\sum_{|\iota|_\infty \leq N} \varpi_\iota \Big(\int_{-1}^{1} I_{\lambda,N} [\sigma(\varrho_\iota,\lambda) F(\mathcal{Z}(\lambda)) - \sigma(\varrho_\iota,\lambda) F(\mathcal{Z}_N(\lambda))] d\lambda \Big)^2 \Big]^{\frac{1}{2}}. \end{aligned} \tag{4.15}$$

We obtain it by using the Cauchy-Schwarz inequality

$$\begin{aligned} \| B_3 \| &\leq \Big[\sum_{|\iota|_\infty \leq N} \varpi_\iota \int_{-1}^{1} I_{\lambda,N} |\sigma(\varrho_\iota,\lambda) F(\mathcal{Z}(\lambda)) - \sigma(\varrho_\iota,\lambda) F(\mathcal{Z}_N(\lambda))|^2 d\lambda \Big]^{\frac{1}{2}} \\ &\leq \Big[\sum_{|\iota|_\infty \leq N} \varpi_\iota \sum_{|\ell|_\infty \leq N} \varpi_\ell |\sigma(\varrho_\iota,\lambda_\ell) F(\mathcal{Z}(\lambda_\ell)) - \sigma(\varrho_\iota,\lambda_\ell) F(\mathcal{Z}_N(\lambda_\ell))|^2 \Big]^{\frac{1}{2}}. \end{aligned} \tag{4.16}$$

By using the Lipschitz condition, we can write

$$\begin{aligned} \| B_3 \| &\leq LM \Big[\sum_{|\iota|_\infty \leq N} \varpi_\iota \sum_{|\ell|_\infty \leq N} |\mathcal{Z}(\lambda_\ell) - \mathcal{Z}_N(\lambda_\ell)|^2 \varpi_\ell \Big]^{\frac{1}{2}} \\ &\leq LM \Big[\int_{-1}^{1} |I_{\lambda,N} (\mathcal{Z}(\lambda) - \mathcal{Z}_N(\lambda))|^2 d\lambda \Big]^{\frac{1}{2}}. \end{aligned} \tag{4.17}$$

Furthermore, by utilizing the triangle inequality, we derive that

$$\| B_3 \| \leq LM \Big[\Big(\int_{-1}^{1} |I_{\lambda,N} \mathcal{Z}(\lambda) - \mathcal{Z}(\lambda))|^2 d\lambda \Big)^{\frac{1}{2}} + \Big(\int_{-1}^{1} |\mathcal{Z}(\lambda) - \mathcal{Z}_N(\lambda))|^2 d\lambda \Big)^{\frac{1}{2}} \Big]. \tag{4.18}$$

Moreover, we can infer from Lemma 4 that

$$\| B_3 \| \leq c \sqrt{\frac{(N-\eta+1)!}{N!}} (N+\eta)^{-(\eta+1)/2} |\mathcal{Z}| + LM \| E_N \| . \tag{4.19}$$

Consequently, the combination of (4.11), (4.14), and (4.19) results in the desired conclusion of this theorem.

5. Numerical results

We examine several examples to validate the proposed methodology's effectiveness and accuracy. The absolute error (AE) is defined as the difference between the exact and measured values of an approximate solution. The programs used in this work are run on a PC with an Intel(R) Core(TM) i7-10510U CPU running 1.80 GHz and 2.30 GHz, with 2.00 GB of RAM, and Mathematica version 12 running the code.

The definition of the absolute error (AEs) is as follows:

$$E(\varrho) = \mid \mathcal{Z}(\varrho) - \mathcal{Z}_{Approx}(\varrho) \mid . \tag{5.1}$$

Where $\mathcal{Z}_{Approx}(\varrho)$ and $\mathcal{Z}(\varrho)$ are the approximate and exact solutions at z, respectively.

Example 1. First, we present non-FFIDEs.

$$\begin{cases} D^{\alpha_1}\mathcal{Z}(\varrho) = F(\varrho) + \int_0^1 (\varrho\lambda + \varrho^2\lambda^2)(\mathcal{Z}(\lambda))^2 d\lambda, \\ \mathcal{Z}(0) = 0. \end{cases} \tag{5.2}$$

While $F(\varrho)$ is derived from the exact solution $\mathcal{Z}(\varrho) = \varrho^3 - \varrho^5$ with $\alpha_1 = 0.9$.

The methodology outlined in Section 3.2 is applied to address the problem. The outcomes presented in Table 1 depict the AE corresponding to various choices of ν_1. The AE for Example 1 is illustrated in Figure 1 for $\nu_1 = 6$, while the AE is illustrated in Figure 2 for $\nu_1 = 12$. Additionally, Figure 3 displays the numerical approximation of $\kappa_{\nu_1}(\varrho)$ for various fractional orders (α_1). From Table 1 and Figures 1 and 2, it is evident that the proposed algorithm yields a highly accurate approximation of the exact solution, even with a minimal number of collocation points. The results highlight the superior accuracy of our method. Taking $\alpha_1 = 0.5$ and $\nu_1 = 12$, we obtain $\mathcal{Z}_{\nu_1}(\varrho)$ of Example 1 as

$$\begin{aligned} \mathcal{Z}_{12}(\varrho) = &- 2.77556 \times 10^{-17} - 6.55032 \times 10^{-15}\varrho + 3.72147 \times 10^{-13}\varrho^2 \\ &+ \varrho^3 + 7.95231 \times 10^{-11}\varrho^4 - \varrho^5 + 1.80595 \times 10^{-9}\varrho^6 \\ &- 4.43547 \times 10^{-9}\varrho^7 + 7.19967 \times 10^{-9}\varrho^8 - 7.65684 \times 10^{-9}\varrho^9 \\ &+ 5.12803 \times 10^{-9}\varrho^{10} - 1.96105 \times 10^{-9}\varrho^{11} + 3.26391 \times 10^{-10}\varrho^{12}. \end{aligned} \tag{5.3}$$

Taking $\alpha_1 = 0.7$ and $\nu_1 = 12$, we obtain $\mathcal{Z}_{\nu_1}(\varrho)$ of Example 1 as

$$\begin{aligned} \mathcal{Z}_{12}(\varrho) = &2.77556 \times 10^{-17} - 1.55431 \times 10^{-15}\varrho + 9.50351 \times 10^{-14}\varrho^2 \\ &+ \varrho^3 + 1.84204 \times 10^{-11}\varrho^4 - \varrho^5 + 3.69927 \times 10^{-10}\varrho^6 \\ &- 8.54932 \times 10^{-10}\varrho^7 + 1.31104 \times 10^{-9}\varrho^8 - 1.32461 \times 10^{-9}\varrho^9 \\ &+ 8.48264 \times 10^{-10}\varrho^{10} - 3.12294 \times 10^{-10}\varrho^{11} + 5.03782 \times 10^{-11}\varrho^{12}. \end{aligned} \tag{5.4}$$

Taking $\alpha_1 = 0.9$ and $\nu_1 = 12$, we obtain $\mathcal{Z}_{\nu_1}(\varrho)$ of Example 1 as

$$\begin{aligned} \mathcal{Z}_{12}(\varrho) = &0. - 4.44089 \times 10^{-15}\varrho + 1.9007 \times 10^{-}13\varrho^2 \\ &+ \varrho^3 + 3.32756 \times 10^{-11}\varrho^4 - \varrho^5 + 7.05267 \times 10^{-10}\varrho^6 \\ &- 1.70713 \times 10^{-9}\varrho^7 + 2.75091 \times 10^{-9}\varrho^8 - 2.91912 \times 10^{-9}\varrho^9 \\ &+ 1.9581 \times 10^{-9}\varrho^{10} - 7.52261 \times 10^{-10}\varrho^{11} + 1.26101 \times 10^{-10}\varrho^{12}. \end{aligned} \tag{5.5}$$

Table 1. AE of Example 1 for $\nu_1 = 6$ and $\nu_1 = 12$.

	$\nu_1 = 6$	$\nu_1 = 12$
0	6.93889×10^{-18}	5.27633×10^{-18}
0.1	6.56823×10^{-11}	3.81986×10^{-17}
0.2	4.33603×10^{-10}	4.69485×10^{-17}
0.3	1.34643×10^{-9}	8.92014×10^{-18}
0.4	3.03353×10^{-9}	2.8328×10^{-17}
0.5	5.71581×10^{-9}	9.45104×10^{-17}
0.6	9.60907×10^{-9}	7.40932×10^{-16}
0.7	1.49258×10^{-8}	2.36254×10^{-16}
0.8	2.18756×10^{-8}	5.14069×10^{-16}
0.9	3.06637×10^{-8}	4.8150×10^{-16}
1.0	4.14886×10^{-8}	4.23968×10^{-16}

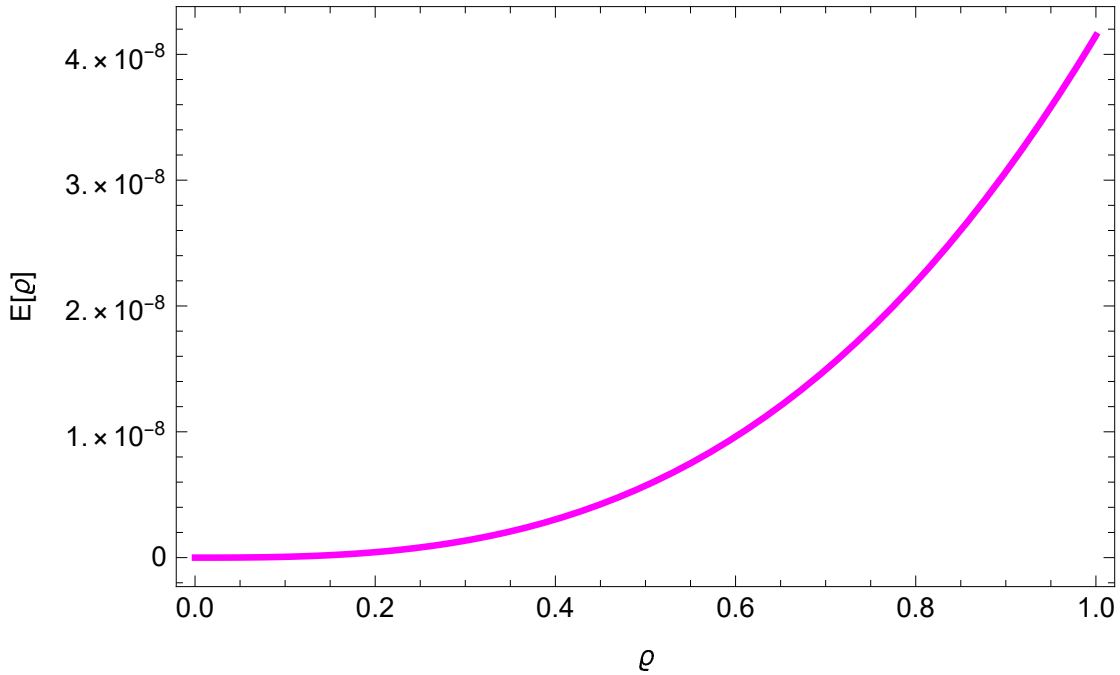

Figure 1. The curve of AE as a function of ϱ in Example 1 is plotted for $\nu_1 = 6$ and $\alpha_1 = 0.9$.

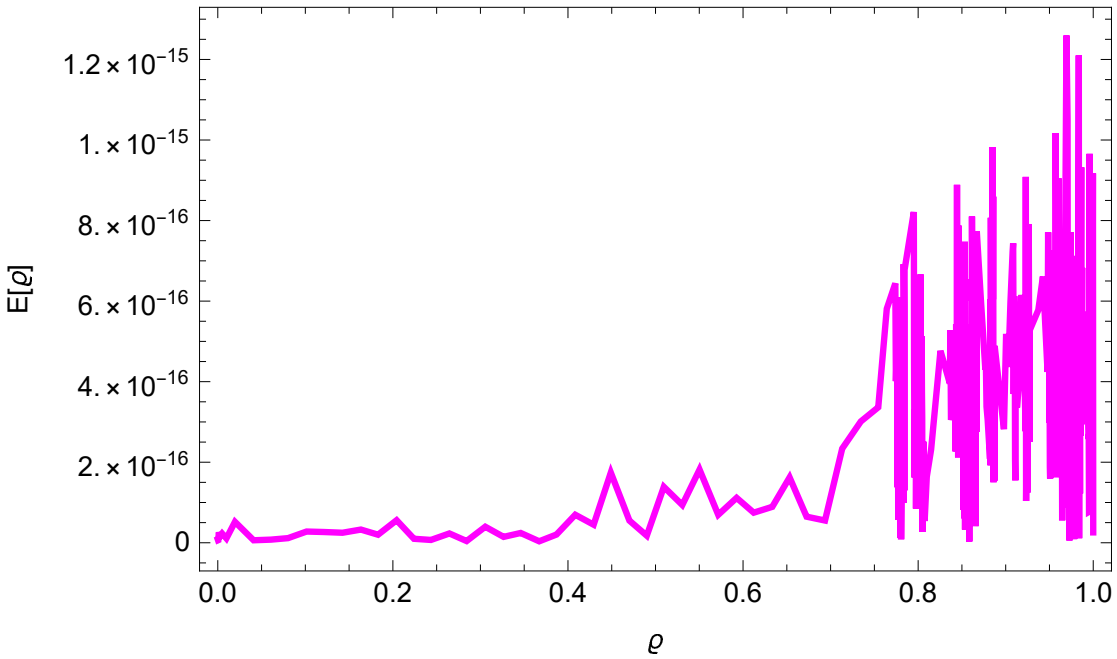

Figure 2. The curve of AE as a function of ϱ in Example 1 is plotted for $\nu_1 = 12$ and $\alpha_1 = 0.9$.

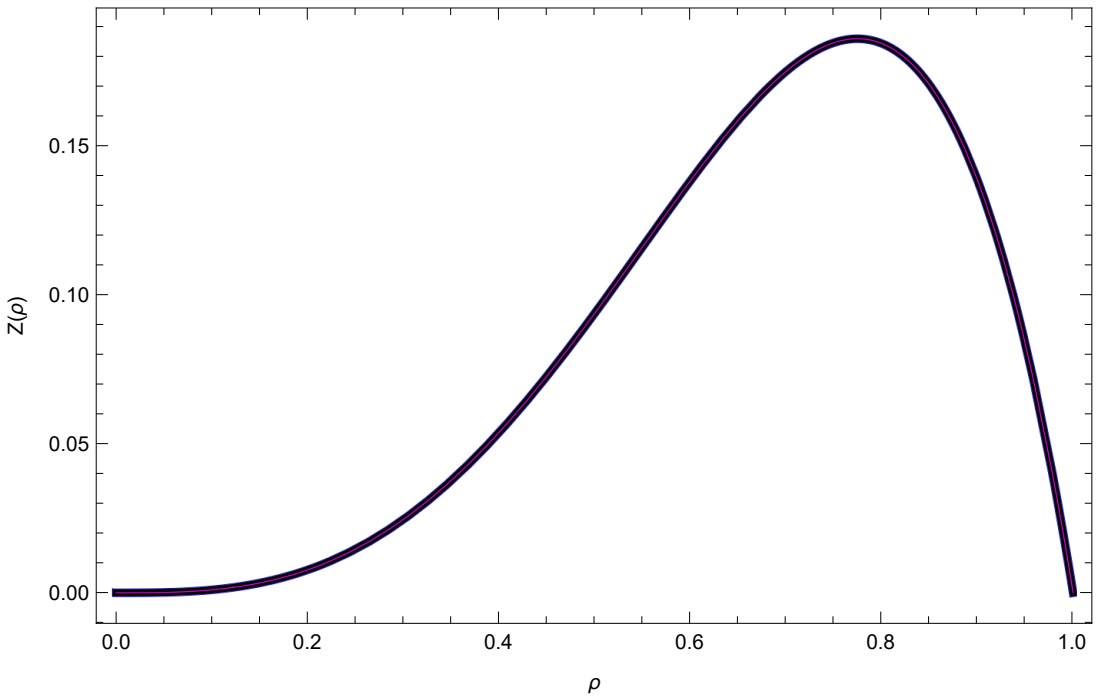

Figure 3. This graph illustrates κ_{ν_1} for Example 1 at fractional orders $\alpha_1 = 0.1, 0.3, 0.5, 0.7, 0.9$, with $\nu_1 = 12$.

Example 2. The following non-FFIDEs are considered [20]:

$$\begin{cases} D^{\alpha_1}\mathcal{Z}(\varrho) = \frac{1}{\Gamma(\frac{1}{2})}(\frac{8}{3}\sqrt{\varrho^3} - 2\sqrt{\varrho}) - \frac{\varrho}{1260} + \int_0^1 \varrho\lambda(\mathcal{Z}(\lambda))^4 d\lambda, \\ \mathcal{Z}(0) = 0, \end{cases} \tag{5.6}$$

where $\alpha_1 = 0.5$ and the exact solution $\mathcal{Z}(\varrho) = \varrho^2 - \varrho$. We examine the convergence and computational processing time of our approach. It is evident that our proposed method outperforms Chebyshev wavelet [20]. Table 2 presents the root mean square errors between Chebyshev wavelet [20] and the current method across different ν_1 values, along with the corresponding CPU time in seconds. Furthermore, in Figure 4, we represent the logarithmic graphs of M_E (i.e., $\log_{10} M_E$) obtained by the proposed method with different values of ν_1. It is demonstrated from the results of this example that the present scheme provides very highly accurate approximation of the solution for the problems and yields accurate convergence rates.

Table 2. Root mean square errors for Example 2 and the corresponding CPU time (in seconds).

Chebyshev wavelet [20]			Present method and CPU time					
$\nu_1 = 8$	$\nu_1 = 16$	$\nu_1 = 32$	$\nu_1 = 8$	*time*	$\nu_1 = 12$	*time*	$\nu_1 = 14$	*time*
6.0×10^{-5}	1.5×10^{-6}	2.3×10^{-7}	2.1×10^{-17}	6.3	1.7×10^{-17}	7.1	1.1×10^{-17}	8.2

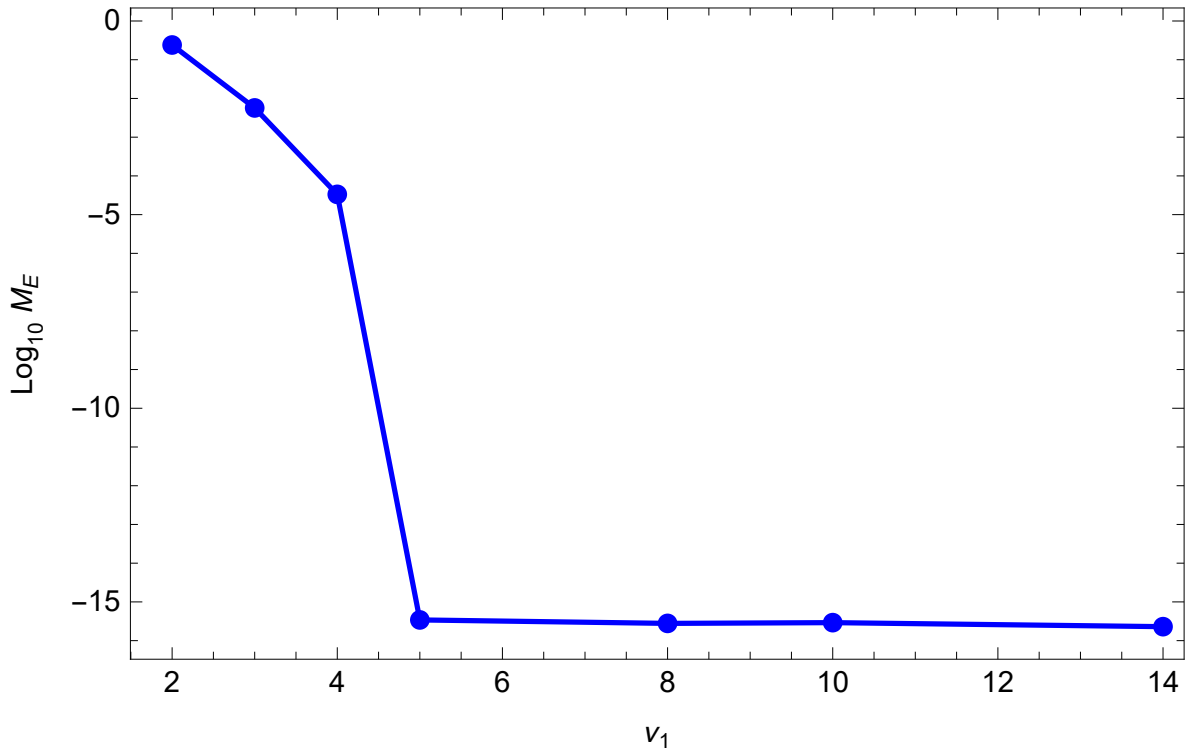

Figure 4. Convergence for Example 2.

Example 3. Consider the following non-FFIDEs:

$$\begin{cases} D^{\alpha_1}\mathcal{Z}(\varrho) = F(\varrho) + \int_0^1 (\varrho + \lambda)^2(\mathcal{Z}(\lambda))^3 d\lambda, \\ \mathcal{Z}(0) = \mathcal{Z}'(0) = 0, \end{cases} \tag{5.7}$$

where F is from exact solution $\mathcal{Z}(\varrho) = \varrho^3 - \varrho^2$.

The outcomes of the L-G-LC method for various ν_1 values are presented in Table 3. In Figure 5, we graph the AE curve of Example 3 for $\nu_1 = 5$ and $\nu_1 = 8$. The concordance between the curves of $\mathcal{Z}(\varrho)$ and $\mathcal{Z}_{Approx}(\varrho)$ from Example 3 is illustrated in Figure 6. From the results, we verify that our scheme reveals superior accuracy, even for just a few points.

Example 4. Consider the following non-FFIDEs

$$\begin{cases} D^{\alpha_1}\mathcal{Z}(\varrho) = F(\varrho) + \int_0^1 (\varrho\lambda)(\mathcal{Z}(\lambda))^2 d\lambda, \\ \mathcal{Z}(0) = 0, \end{cases} \tag{5.8}$$

where F is from exact solution $\mathcal{Z}(\varrho) = e^{-0.5\varrho} sin(\pi\varrho)$.

The outcomes of the L-G-LC method for various ν_1 values are displayed in Table 4. Furthermore, in Figure 7, we depict the logarithmic graphs of M_E (i.e., $\log_{10} M_E$) obtained by the proposed method for various values of ν_1 and $\alpha_1 = 0.2, 0.5, 0.9$. Thus, we have illustrated that the present method offers a precise approximation for problems characterized by nonlinearity and lack of smoothness.

Table 3. AE of Example 3 for $\nu_1 = 5$ and $\nu_1 = 8$.

	$\nu_1 = 5$	$\nu_1 = 8$
0.1	9.47702×10^{-7}	1.76628×10^{-17}
0.2	2.45058×10^{-6}	2.71915×10^{-17}
0.3	3.44428×10^{-6}	3.75761×10^{-17}
0.4	3.80608×10^{-6}	5.33192×10^{-17}
0.5	3.95518×10^{-6}	5.39188×10^{-17}
0.6	4.45308×10^{-6}	1.71356×10^{-16}
0.7	5.60389×10^{-6}	1.69977×10^{-16}
0.8	7.05468×10^{-6}	1.83947×10^{-16}
0.9	7.39584×10^{-6}	1.96828×10^{-16}
1.0	3.76138×10^{-6}	2.73561×10^{-16}

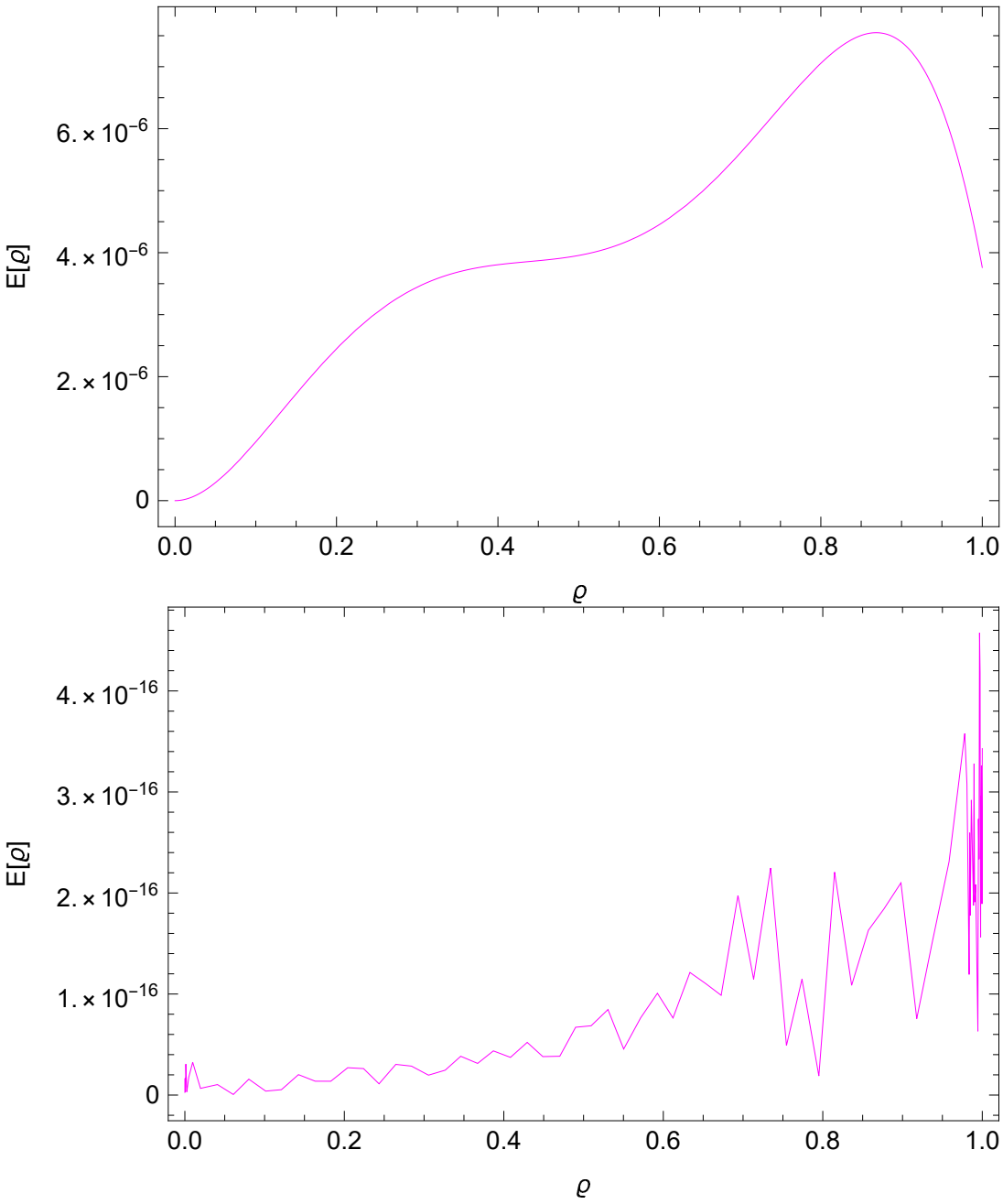

Figure 5. The AE curve versus ϱ in Example 3 for $\alpha = 0.5$, and $\nu_1 = 5$ and $\nu_1 = 8$, respectively.

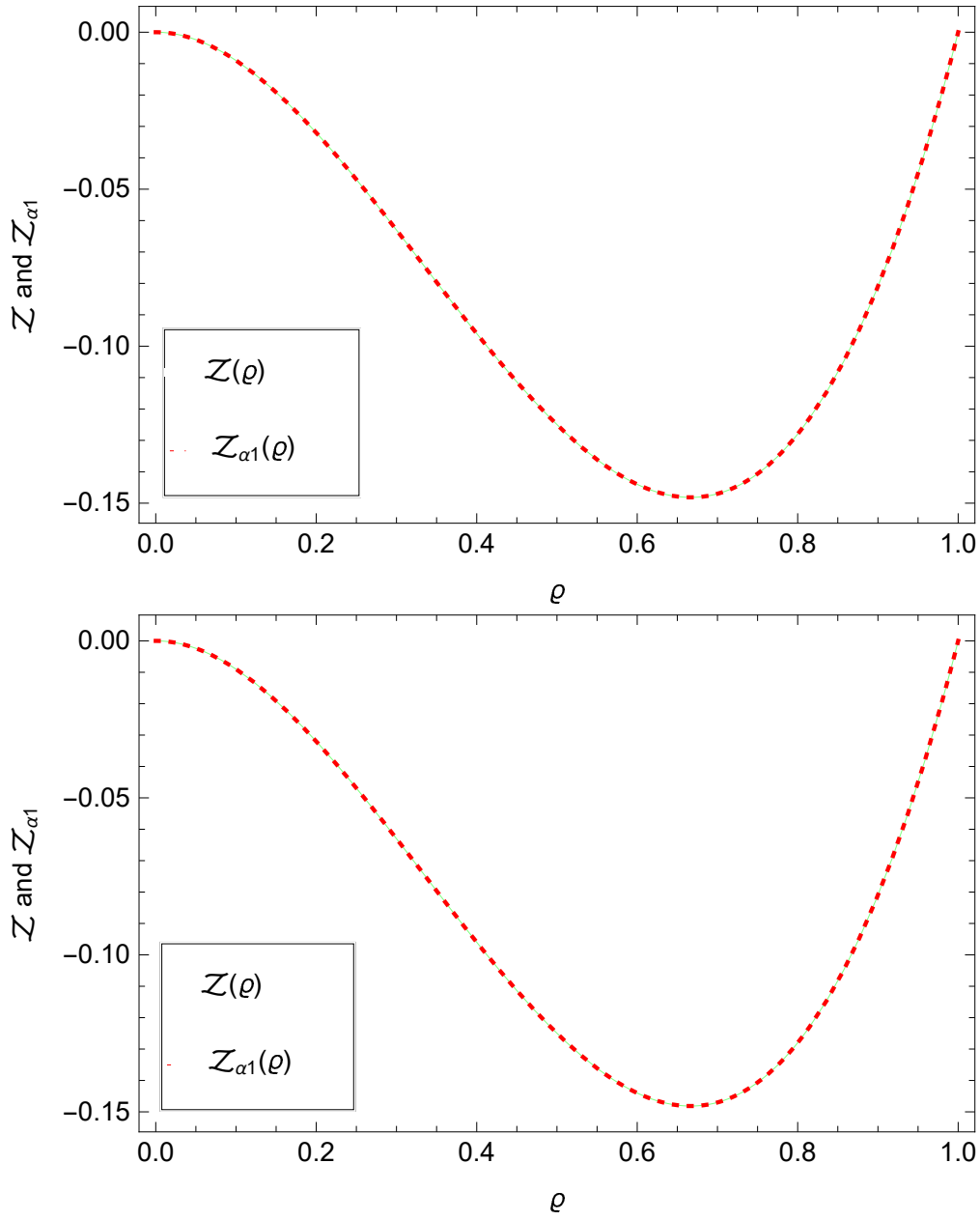

Figure 6. The $\mathcal{Z}_{Approx}(\varrho)$ and $\mathcal{Z}(\varrho)$ for Example 3 when for $\nu_1 = 5$ and $\nu_1 = 8$, respectively.

Table 4. Maximum absolute error (MAE) of Example 4 for $\nu_1 = 6$, $\nu_1 = 8$, $\nu_1 = 10$, $\nu_1 = 14$.

ν_1	$\nu_1 = 6$	$\nu_1 = 8$	$\nu_1 = 10$	$\nu_1 = 14$
MAX	8.3×10^{-5}	8.07×10^{-7}	4.65×10^{-9}	4.17×10^{-14}

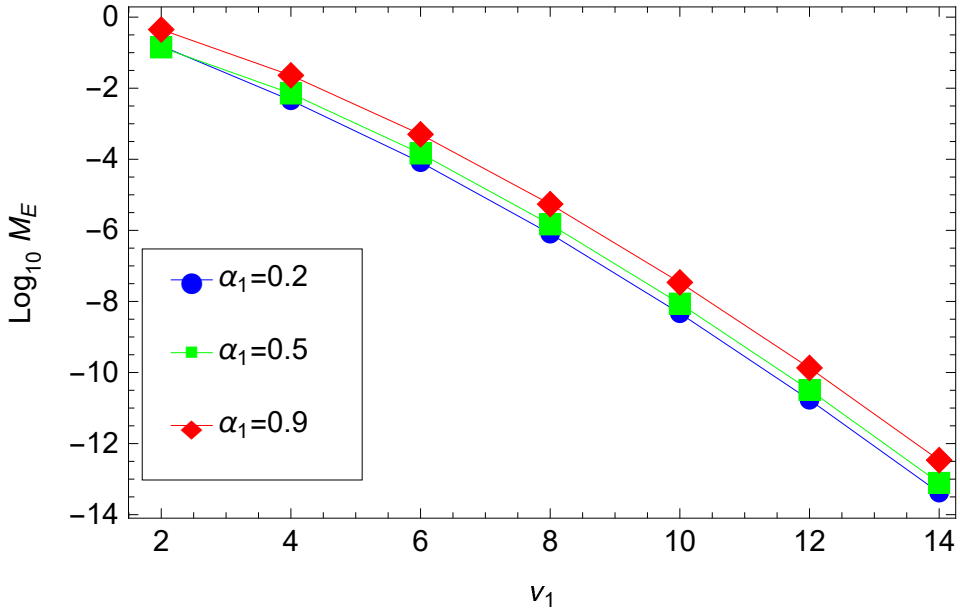

Figure 7. Convergence for Example 4.

Example 5. Finally, we present non-FFIDEs.

$$\begin{cases} D^{\alpha_1}\mathcal{Z}(\varrho) = 1 - \frac{\varrho}{4} + \int_0^1 (\varrho\lambda)(\mathcal{Z}(\lambda))^2 d\lambda, \\ \mathcal{Z}(0) = 0, \end{cases} \tag{5.9}$$

where the exact solution $\mathcal{Z}(\varrho) = \varrho$ for $\alpha_1 = 1$.

Table 5 exhibits the root mean square errors with $\alpha_1 = 1$. The exact and approximate solutions are graphed in Figure 8 for $\alpha_1 = 1$. Figure 9–12 show the AE curve versus ϱ in Example 5 for $\nu_1 = 12$ with various $\alpha_1 = 0.25, 0.5, 0.75, 1$, respectively. Moreover, in the absence of exact solutions, we have plotted the approximate solutions for various values of α_1. The results show that our technique achieves greater accuracy, even for a few points.

Table 5. Root mean square errors of Example 5.

Second kind Chebyshev wavelet [20]			
$(k = 3, M = 2)$	$(k = 4, M = 2)$	$(k = 5, M = 2)$	$(k = 4, M = 1)$
$2.9700e^{-007}$	$1.8610e^{-008}$	$1.1645e^{-009}$	$1.6745e^{-005}$
Our method at different values of ν_1			
4	6	8	12
5.12745×10^{-17}	4.23208×10^{-17}	4.95392×10^{-18}	3.54902×10^{-18}

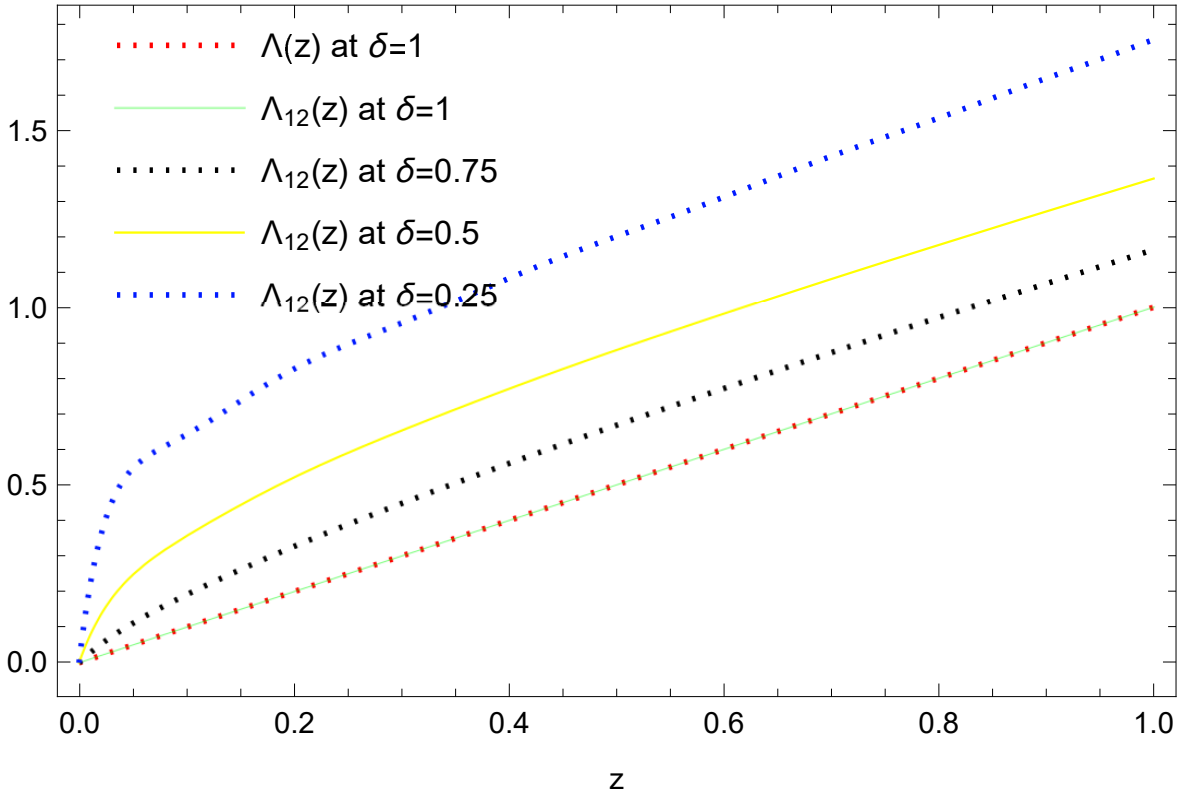

Figure 8. The approximate solutions for various values of α_1.

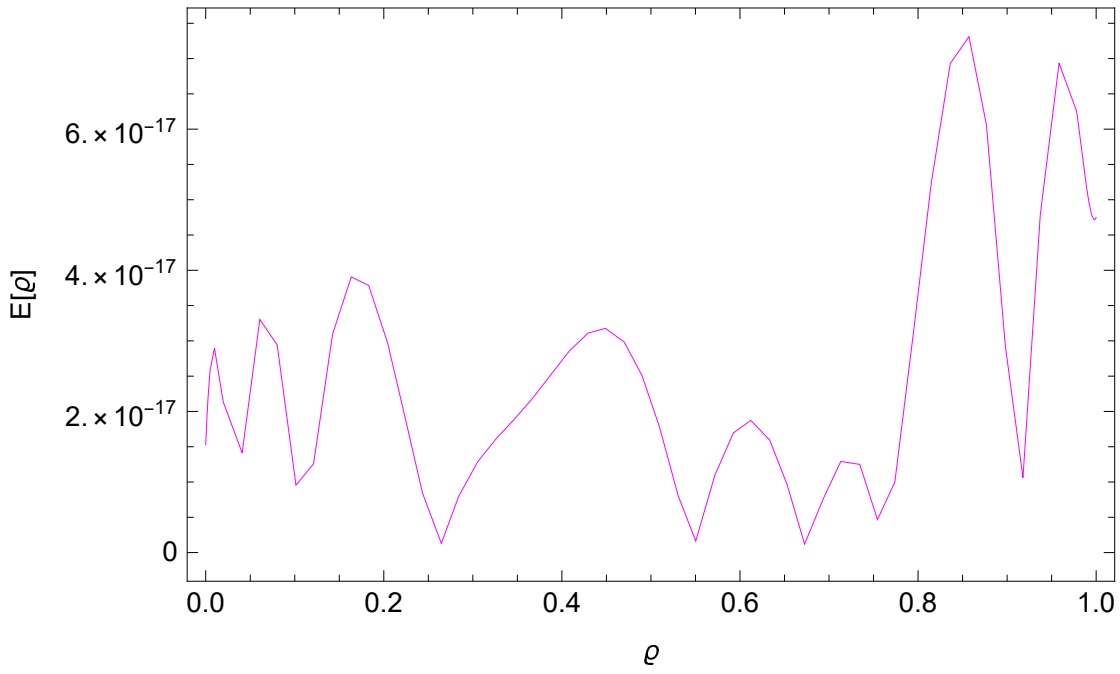

Figure 9. The AE curve versus ϱ in Example 5 for $\nu_1 = 12$ and $\alpha_1 = 0.25$.

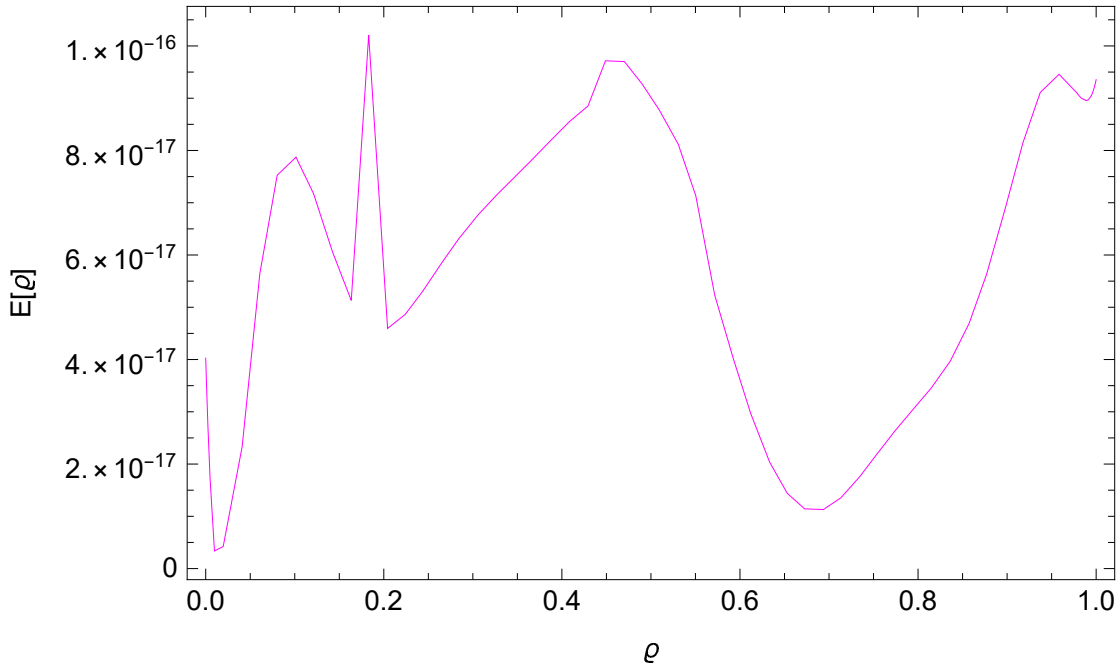

Figure 10. The AE curve versus ϱ in Example 5 for $\nu_1 = 12$ and $\alpha_1 = 0.5$.

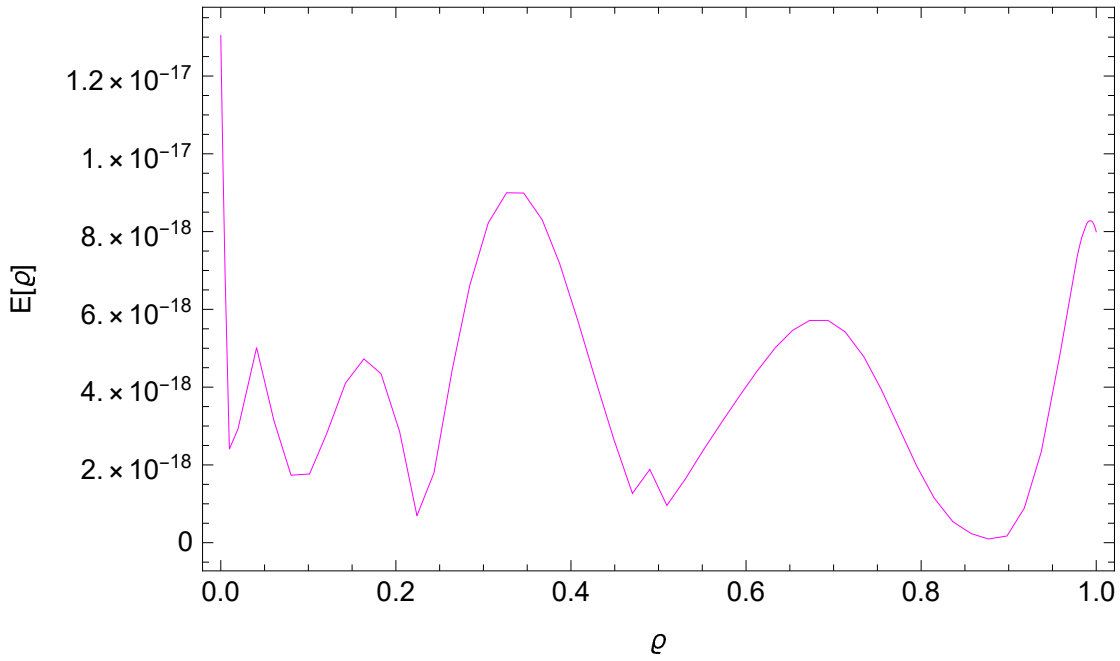

Figure 11. The AE curve versus ϱ in Example 5 for $\nu_1 = 12$ and $\alpha_1 = 0.75$.

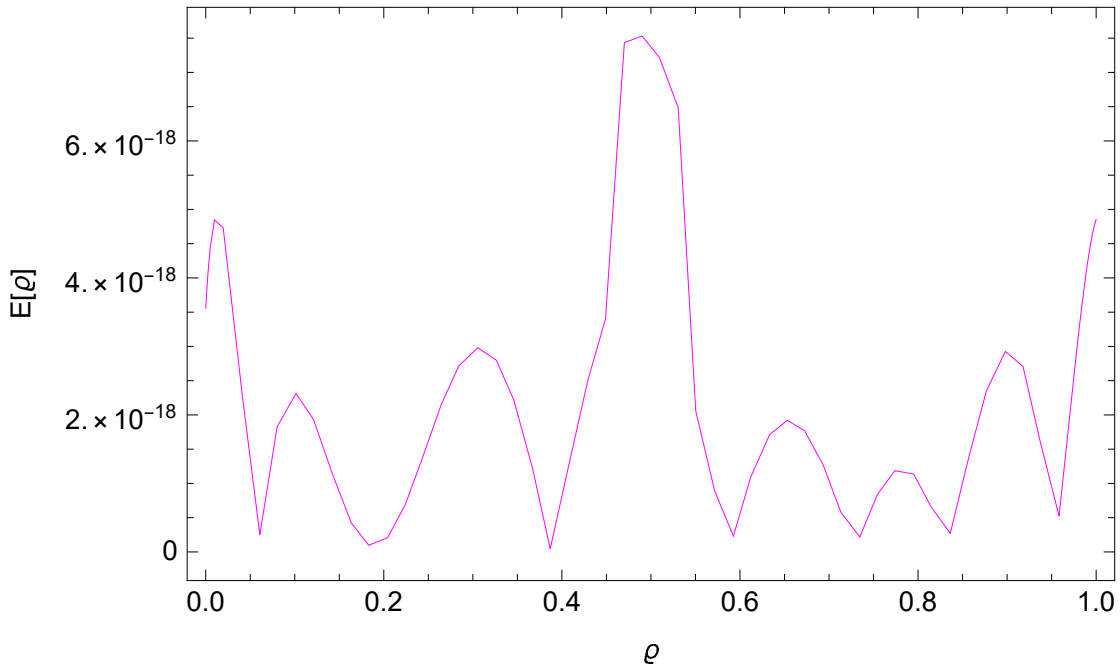

Figure 12. The AE curve versus ϱ in Example 5 for $\nu_1 = 12$ and $\alpha_1 = 1$.

Example 6. The following non-FFIDE with non-smooth solution is considered [53]:

$$\begin{cases} D^{\frac{1}{2}}\mathcal{Z}(\varrho) = \frac{\sqrt{\pi}}{2} - \frac{1}{4} + \frac{1}{2}\int_0^1 (\mathcal{Z}(\lambda))^2 d\lambda, \\ \mathcal{Z}(0) = 0, \end{cases} \tag{5.10}$$

where the exact solution $\mathcal{Z}(\varrho) = \sqrt{\varrho}$.

Figure 13 presents the AE of Example 6 for $\alpha_1 = \frac{1}{2}$ and ν_1. Figure 14 compares the exact and approximate solutions. We applied our technique by using fractional-order in this example with a non-smooth solution and we can see from the outcomes that the suggested scheme yields superior accuracy. Additionally, it should be noted that good approximations can be made with only a few points.

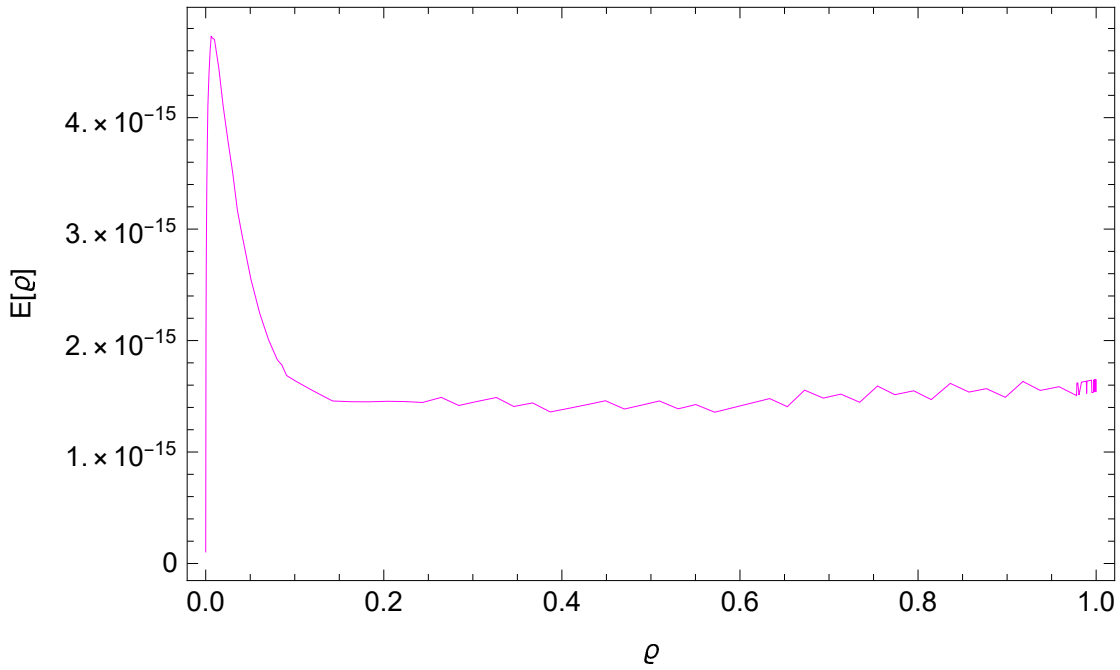

Figure 13. The curve of AE as a function of ϱ in Example 6 is plotted for $\nu_1 = \frac{1}{2}$.

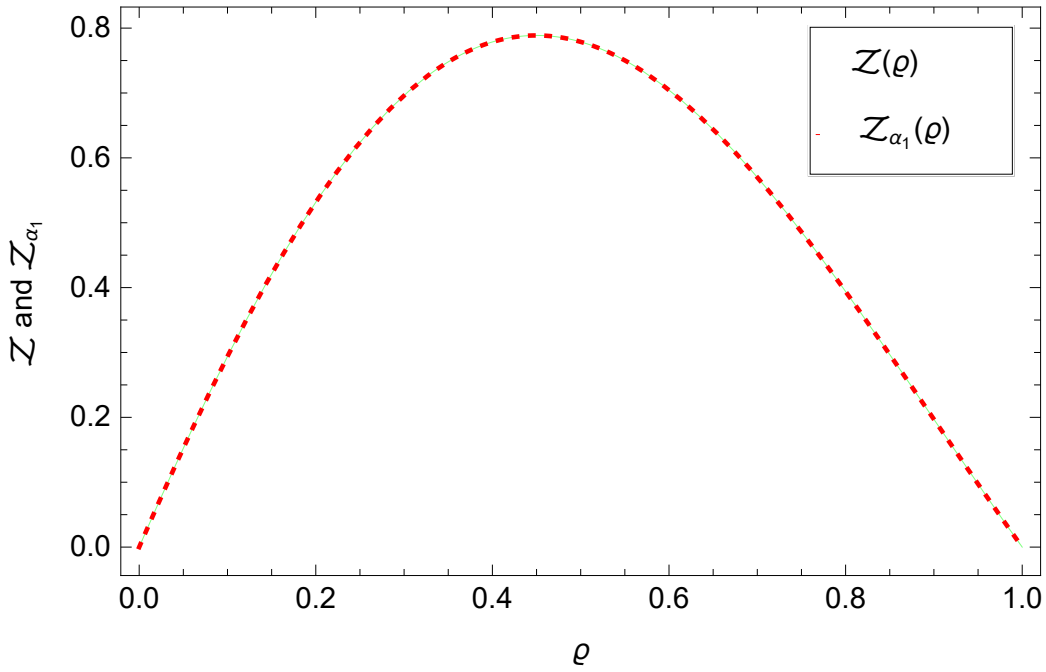

Figure 14. The $\mathcal{Z}_{Approx}(\varrho)$ and $\mathcal{Z}(\varrho)$ for Example 6 for $\nu_1 = \frac{1}{2}$.

Example 7. Consider the following non-FFIDE with non-smooth solution [53]:

$$\begin{cases} D^{\frac{1}{2}}\mathcal{Z}(\varrho) = F(\varrho) + \int_0^1 sin(\varrho + \lambda)(\mathcal{Z}(\lambda))^2 d\lambda, \\ \mathcal{Z}(0) = 0, \end{cases} \tag{5.11}$$

where $F(\varrho)$ is obtained from the exact solution $\mathcal{Z}(\varrho) = \varrho^{\frac{1}{2}} - \frac{1}{3!}\varrho^{\frac{3}{2}} + \frac{1}{5!}\varrho^{\frac{5}{2}}$.

For our algorithm, we get the maximum errors shown in Table 6, for various values of α_1 and ν_1. In Table 6 we compare our method with the approach presented in [53], in terms of the MAE. From the results, we verify that our scheme reveals superior accuracy, even for just a few points.

Table 6. MAE of Example 7 at different values of ν_1.

Method in [53]			
$(\nu 1 = 20, \alpha 1 = \frac{1}{4})$	$(\nu 1 = 20, \alpha 1 = \frac{1}{2})$	$(\nu 1 = 20, \alpha 1 = \frac{3}{4})$	$(\nu 1 = 20, \alpha 1 = 1)$
$3.6870e^{-14}$	$1.5224e^{-20}$	$5.8209e^{-03}$	$2.3830e^{-02}$
Our method			
$(\nu 1 = 8, \alpha 1 = \frac{1}{4})$	$(\nu 1 = 8, \alpha 1 = \frac{1}{2})$	$(\nu 1 = 8, \alpha 1 = \frac{3}{4})$	$(\nu 1 = 8, \alpha 1 = 1)$
2.98244×10^{-14}	1.5576×10^{-14}	5.64913×10^{-15}	1.15437×10^{-02}

6. Conclusions

In this study, we introduce a precise and efficient numerical algorithm based on the L-G-LC method to solve non-FFIDEs with initial value problems. The resolution of the nonlinear algebraic equations system was employed to solve the problem. Utilizing the LGL points as collocation nodes in the approximate solution preserves spectral convergence for the spatial variable. To illustrate the efficacy of the derived numerical algorithm, numerical examples were presented. The algorithm demonstrates efficiency, applicability to various operators, and extensibility to multi-dimensional problems, laying the foundation for future research. In subsequent investigations, we aim to address fractional integro-differential equations involving generalized formulations.

In conclusion, based on the theoretical formulation and numerical illustrations, we confirm that:

(1) The presented method yields accurate and reliable solutions, when compared with other approaches.

(2) The error decays exponentially as $\nu_1 \to \infty$ in the case of smooth solutions.

(3) An upper bound for the absolute error in the approximate solution can be determined.

(4) If the solution is not smooth, then the order of convergence of the numerical scheme may deteriorate. However, this can be prevented by using fractional order Legendre functions.

Furthermore, we will study in the future a variable-order and stochastic fractional integro-differential equation with a non-smooth solution by utilizing a combination of the finite difference and spectral methods.

Use of AI tools declaration

The authors declare they have not used Artificial Intelligence (AI) tools in the creation of this article.

Acknowledgments

The authors extend their appreciation to the Deanship of Scientific Research at King Khalid University for funding this work through Large Research Group project under grant number (R.G.P. 2/81/44).

Conflict of interest

The authors declare no conflicts of interest.

References

1. L. Guo, X. L. Zhao, X. M. Gu, Y. L. Zhao, Y. B. Zheng, T. Z. Huang, Three-dimensional fractional total variation regularized tensor optimized model for image deblurring, *Appl. Math. Comput.*, **404** (2021), 126224. https://doi.org/10.1016/j.amc.2021.126224
2. K. S. Miller, B. Ross, *An introduction to the fractional calculus and fractional differential equations*, Wiley, 1993.
3. Y. Y. Huang, X. M. Gu, Y. Gong, H. Li, Y. L. Zhao, B. Carpentieri, A fast preconditioned semi-implicit difference scheme for strongly nonlinear space-fractional diffusion equations, *Fractal Fract.*, **5** (2021), 230. https://doi.org/10.3390/fractalfract5040230
4. X. M. Gu, H. W. Sun, Y. L. Zhao, X. C. Zheng, An implicit difference scheme for time-fractional diffusion equations with a time-invariant type variable order, *Appl. Math. Lett.*, **120** (2021),107270. https://doi.org/10.1016/j.aml.2021.107270
5. W. H. Luo, C. P. Li, T. Z. Huang, X. M. Gu, G. C. Wu, A high-order accurate numerical scheme for the caputo derivative with applications to fractional diffusion problems, *Numer. Func. Anal. Opt.*, **39** (2018), 600–622. https://doi.org/10.1080/01630563.2017.1402346
6. V. P. Dubey, J. Singh, S. Dubey, D. Kumar, Analysis of Cauchy problems and diffusion equations associated with the Hilfer-Prabhakar fractional derivative via Kharrat-Toma transform, *Fractal Fract.*, **7** (2023), 413. https://doi.org/10.3390/fractalfract7050413
7. J. Singh, R. Agrawal, K. S. Nisar, A new forecasting behavior of fractional model of atmospheric dynamics of carbon dioxide gas, *Part. Differ. Equ. Appl. Math.*, **9** (2024), 100595. https://doi.org/10.1016/j.padiff.2023.100595
8. J. Singh, A. M. Alshehri, Sushila, D. Kumar, Computational analysis of fractional liénard's equation with exponential memory, *J. Comput. Nonlin. Dyn.*, **18** (2023), 041004. https://doi.org/10.1115/1.4056858
9. O. Martin, On the homotopy analysis method for solving a particle transport equation, *Appl. Math. Model.*, **37** (2013), 3959–3967. https://doi.org/10.1016/j.apm.2012.08.023

10. Z. Jackiewicz, M. Rahman, B. D. Welfert, Numerical solution of a Fredholm integro-differential equation modelling θ-neural networks, *Appl. Math. Comput.*, **195** (2008), 523–536. https://doi.org/10.1016/j.icarus.2007.12.026
11. Ş. Yüzbaşı, M. Sezer, B. Kemancı, Numerical solutions of integro-differential equations and application of a population model with an improved legendre method, *Appl. Math. Model.*, **37** (2013), 2086–2101. https://doi.org/10.1016/j.apm.2012.05.012
12. N. Hale, An ultraspherical spectral method for linear Fredholm and Volterra integro-differential equations of convolution type, *IMA J. Numer. Anal.*, **39** (2019), 1727–1746. https://doi.org/10.1093/imanum/dry042
13. N. Koshev, L. Beilina, An adaptive finite element method for Fredholm integral equations of the first kind and its verification on experimental data, *Open Math.*, **11** (2013), 1489–1509. https://doi.org/10.2478/s11533-013-0247-3
14. J. Medlock, M. Kot, Spreading disease: Integro-differential equations old and new, *Math. Biosci.*, **184** (2003), 201–222. https://doi.org/10.1016/S0025-5564(03)00041-5
15. M. R. Eslahchi, M. Dehghan, M. Parvizi, Application of the collocation method for solving nonlinear fractional integro-differential equations, *J. Comput. Appl. Math.*, **257** (2014), 105–128. https://doi.org/10.1016/j.cam.2013.07.044
16. H. Li, Y. Jiang, Z. Wang, L. Zhang, Z. Teng, Global Mittag-Leffler stability of coupled system of fractional-order differential equations on network, *Appl. Math. Comput.*, **270** (2015), 269–277. https://doi.org/10.1016/j.amc.2015.08.043
17. M. Gülsu, Y. Öztürk, A. Anapalı, Numerical approach for solving fractional Fredholm integro-differential equation, *Int. J. Comput. Math.*, **90** (2013), 1413–1434. https://doi.org/10.1080/00207160.2012.750720
18. A. Darweesh, M. Alquran, K. Aghzawi, New numerical treatment for a family of two-dimensional fractional Fredholm integro-differential equations, *Algorithms*, **13** (2020), 37. https://doi.org/10.3390/a13020037
19. W. Jiang, T. Tian, Numerical solution of nonlinear Volterra integro-differential equations of fractional order by the reproducing kernel method, *Appl. Math. Model.*, **39** (2015), 4871–4876. https://doi.org/10.1016/j.apm.2015.03.053
20. L. Zhu, Q. Fan, Solving fractional nonlinear Fredholm integro-differential equations by the second kind Chebyshev wavelet, *Commun. Nonlinear Sci.*, **17** (2012), 2333–2341. https://doi.org/10.1016/j.cnsns.2011.10.014
21. I. Aziz, M. Fayyaz, A new approach for numerical solution of integro-differential equations via Haar wavelets, *Int. J. Comput. Math.*, **90** (2013), 1971–1989. https://doi.org/10.1080/00207160.2013.770481
22. B. K. Mousavi, M. H. Heydari, Wilson wavelets method for solving nonlinear fractional Fredholm-Hammerstein integro-differential equations, *Int. J. Comput. Math.*, **97** (2020), 2165–2177. https://doi.org/10.1080/00207160.2019.1683731
23. L. Huang, X. F. Li, Y. L. Zhao, X. Y. Duan, Approximate solution of fractional integro-differential equations by Taylor expansion method, *Comput. Math. Appl.*, **62** (2011), 1127–1134. https://doi.org/10.1016/j.camwa.2011.03.037

24. X. M. Gu, S. L. Wu, A parallel-in-time iterative algorithm for Volterra partial integro-differential problems with weakly singular kernel, *J. Comput. Phys.*, **417** (2020), 109576. https://doi.org/10.1016/j.jcp.2020.109576
25. X. Ma, C. Huang, Spectral collocation method for linear fractional integro-differential equations, *Appl. Math. Model.*, **38** (2014), 1434–1448. https://doi.org/10.1016/j.apm.2013.08.013
26. F. Yousefi, A. Rivaz, W. Chen, The construction of operational matrix of fractional integration for solving fractional differential and integro-differential equations, *Neural Comput. Appl.*, **31** (2019), 1867–1878. https://doi.org/10.1007/s00521-017-3163-9
27. E. H. Doha, M. A. Abdelkawy, A. Z. M. Amin, D. Baleanu, Shifted Jacobi spectral collocation method with convergence analysis for solving integro-differential equations and system of integro-differential equations, *Nonlinear Anal.-Model.*, **24** (2019), 332–352. https://doi.org/10.15388/NA.2019.3.2
28. K. Maleknejad, Y. Mahmoudi, Taylor polynomial solution of high-order nonlinear Volterra-Fredholm integro-differential equations, *Appl. Math. Comput.*, **145** (2003), 641–653. https://doi.org/10.1016/S0096-3003(03)00152-8
29. A. Pedas, M. Vikerpuur, Spline collocation for multi-term fractional integro-differential equations with weakly singular kernels, *Fractal Fract.*, **5** (2021), 90. https://doi.org/10.3390/fractalfract5030090
30. R. Koundal, R. Kumar, R. Kumar, K. Srivastava, D. Baleanu, A novel collocated-shifted Lucas polynomial approach for fractional integro-differential equations, *Int. J. Appl. Comput. Math.*, **7** (2021), 1–19. https://doi.org/10.1007/s40819-021-01108-0
31. L. Wu, Z. Chen, X. Ding, A minimal search method for solving fractional integro-differential equations based on modified Legendre multiwavelets, *J. Appl. Math. Comput.*, **68** (2022), 1467–1483. https://doi.org/10.1007/s12190-021-01573-2
32. R. Amin, K. Shah, M. Asif, I. Khan, F. Ullah, An efficient algorithm for numerical solution of fractional integro-differential equations via Haar wavelet, *J. Comput. Appl. Math.*, **381** (2021), 113028. https://doi.org/10.1016/j.cam.2020.113028
33. H. Jafari, N. A. Tuan, R. M. Ganji, A new numerical scheme for solving pantograph type nonlinear fractional integro-differential equations, *J. King Saud Univ. Sci.*, **33** (2021), 101185. https://doi.org/10.1016/j.jksus.2020.08.029
34. N. Ford, M. Morgado, M. Rebelo, Nonpolynomial collocation approximation of solutions to fractional differential equations, *Fract. Calc. Appl. Anal.*, **16** (2013), 874–891. https://doi.org/10.2478/s13540-013-0054-3
35. K. Du, On well-conditioned spectral collocation and spectral methods by the integral reformulation, *SIAM J. Sci. Comput.*, **38** (2016), A3247–A3263. https://doi.org/10.1137/15M1046629
36. G. L. Delzanno, Multi-dimensional, fully-implicit, spectral method for the Vlasov-Maxwell equations with exact conservation laws in discrete form, *J. Comput. Phys.*, **301** (2015), 338–356. https://doi.org/10.1016/j.jcp.2015.07.028
37. Y. Chen, J. Zhou, Error estimates of spectral Legendre-Galerkin methods for the fourth-order equation in one dimension, *Appl. Math. Comput.*, **268** (2015), 1217–1226. https://doi.org/10.1016/j.amc.2015.06.082

38. M. A. Abdelkawy, A. Z. M. Amin, A. M. Lopes, Fractional-order shifted Legendre collocation method for solving non-linear variable-order fractional Fredholm integro-differential equations, *Comput. Appl. Math.*, **41** (2022), 1–21. https://doi.org/10.1007/s40314-021-01702-4
39. E. H. Doha, M. A. Abdelkawy, A. Z. M. Amin, D. Baleanu, Spectral technique for solving variable-order fractional Volterra integro-differential equations, *Numer. Meth. Part. D. E.*, **34** (2018), 1659–1677. https://doi.org/10.1002/num.22233
40. A. Z. Amin, M. A. Abdelkawy, E. Solouma, I. Al-Dayel, A spectral collocation method for solving the non-linear distributed-order fractional Bagley-Torvik differential equation, *Fractal Fract.*, **7** (2023), 780. https://doi.org/10.3390/fractalfract7110780
41. A. Z. Amin, A. M. Lopes, I. Hashim, A space-time spectral collocation method for solving the variable-order fractional Fokker-Planck equation, *J. Appl. Anal. Comput.*, **13** (2023), 969–985. https://doi.org/10.11948/20220254
42. E. H. Doha, M. A. Abdelkawy, A. Z. M. Amin, A. M. Lopes, Shifted Jacobi-Gauss-collocation with convergence analysis for fractional integro-differential equations, *Commun. Nonlinear Sci.*, **72** (2019), 342–359. https://doi.org/10.1016/j.cnsns.2019.01.005
43. A. Z. Amin, M. A. Abdelkawy, E. Soluma, M. M. Babatin, A space-time spectral approximation for solving two dimensional variable-order fractional convection-diffusion equations with nonsmooth solutions, *Int. J. Mod. Phys. C*, 2023. https://doi.org/10.1142/S0129183124500888
44. M. A. Abdelkawy, A. Z. M. Amin, A. H. Bhrawy, J. A. T. Machado, A. M. Lopes, Jacobi collocation approximation for solving multi-dimensional Volterra integral equations, *Int. J. Nonlinear Sci.*, **18** (2017), 411–425. https://doi.org/10.1515/ijnsns-2016-0160
45. S. S. Ezz-Eldien, On solving systems of multi-pantograph equations via spectral tau method, *Appl. Math. Comput.*, **321** (2018), 63–73. https://doi.org/10.1016/j.amc.2017.10.014
46. D. D. Hu, Y. Y. Fu, W. J. Cai, Y. S. Wang, Unconditional convergence of conservative spectral Galerkin methods for the coupled fractional nonlinear Klein-Gordon-Schrödinger equations, *J. Sci. Comput*, **94** (2023), 70. https://doi.org/10.1007/s10915-023-02108-6
47. E. H. Doha, A. H. Bhrawy, R. M. Hafez, A Jacobi-Jacobi dual-petrov-Galerkin method for third-and fifth-order differential equations, *Math. Comput. Model.*, **53** (2011), 1820–1832. https://doi.org/10.1016/j.mcm.2011.01.002
48. X. Tang, Efficient Chebyshev collocation methods for solving optimal control problems governed by Volterra integral equations, *Appl. Math. Comput.*, **269** (2015), 118–128. https://doi.org/10.1016/j.amc.2015.07.055
49. M. A. Abdelkawy, A. Z. M. Amin, A. M. Lopes, I. Hashim, M. M. Babatin, Shifted fractional-order Jacobi collocation method for solving variable-order fractional integro-differential equation with weakly singular kernel, *Fractal Fract.*, **6** (2021), 19. https://doi.org/10.3390/fractalfract6010019
50. E. H. Doha, M. A. Abdelkawy, A. Z. M. Amin, A. M. Lopes, On spectral methods for solving variable-order fractional integro-differential equations, *Comput. Appl. Math.*, **37** (2018), 3937–3950. https://doi.org/10.1007/s40314-017-0551-9
51. J. Shen, T. Tang, L. Wang, *Spectral methods: Algorithms, analysis and applications*, Springer Science & Business Media, **41** (2011).
52. C. Canuto, M. Y. Hussaini, A. Quarteroni, T. A. Zang, *Spectral methods: Fundamentals in single domains*, Springer Science & Business Media, 2007.

53. Y. Talaei, S. Noeiaghdam, H. Hosseinzadeh, Numerical solution of fractional order Fredholm integro-differential equations by spectral method with fractional basis functions, *B. Irkutsk State U. M.*, **45** (2023), 89–103. https://doi.org/10.26516/1997-7670.2023.45.89

AIMS Press

© 2024 the Author(s), licensee AIMS Press. This is an open access article distributed under the terms of the Creative Commons Attribution License (http://creativecommons.org/licenses/by/4.0)